Published in final edited form as:
â *Mol Cell Neurosci*. 2007 April ; 34(4): 662â678.

The Atypical Cadherin Flamingo Regulates Synaptogenesis and Helps Prevent Axonal and Synaptic Degeneration in *Drosophila*

Hong Bao[1,#], **Monica L. Berlanga**[2,3,#], **Mingshan Xue**[1,2,&], **Sara M. Hapip**[1], **Richard W. Daniels**[1,**], **John M. Mendenhall**[1], **Adriana A. Alcantara**[2,3], and **Bing Zhang**[1,2,*]

1 *Section of Neurobiology, the University of Texas at Austin, Austin, TX 78712*

2 *Institute for Neuroscience, the University of Texas at Austin, Austin, TX 78712*

3 *Department of Psychology, the University of Texas at Austin, Austin, TX 78712*

Abstract

The formation of synaptic connections with target cells and maintenance of axons are highly regulated and crucial for neuronal function. The atypical cadherin and G-protein-coupled receptor Flamingo and its orthologs in amphibians and mammals have been shown to regulate cell polarity, dendritic and axonal growth, and neural tube closure. However, the role of Flamingo in synapse formation and function and in axonal health remains poorly understood. Here we show that *fmi* mutations cause a significant increase in the number of ectopic synapses on muscles and result in the formation of novel *en passant* synapses along axons, and unique presynaptic varicosities, including active zones, within axons. *fmi* mutations also cause defective synaptic responses in a small subset of muscles, an age-dependent loss of muscle innervation and a drastic degeneration of axons in 3rd instar larvae without an apparent loss of neurons. Neuronal expression of Flamingo rescues all of these synaptic and axonal defects and larval lethality. Based on these observations, we propose that Flamingo is required in neurons for synaptic target selection, synaptogenesis, the survival of axons and synapses, and adult viability. These findings shed new light on a possible role for Flamingo in progressive neurodegenerative diseases.

Keywords

Atypical cadherin; synapse formation; axonal atrophy; neurodegeneration

Introduction

The function of the nervous system depends on the synaptic connections formed and maintained between individual neurons. Axonal targeting and synapse formation are complex cellular processes, requiring that a neuron project along the correct pathway, choose the appropriate target, and construct and maintain a functional synapse (Tessier-Lavigne and

[#]These authors contributed equally to the work.
[&]Current address: Neuroscience Program, Baylor College of Medicine, One Baylor Plaza, Houston, Texas
[**]Current address: Dept. of Molecular Biology and Pharmacology, Washington University School of Medicine, St. Louis, MO 63110.
[*]Please address correspondence to Dr. Bing Zhang Phone: 512-232-7074; Fax: 512-471-9651 Email: bzhang@mail.utexas.edu

Author contributions: HB, MLB, MX, and BZ conceived and designed the experiments. HB, MLB, MX, SMH, RWD, JMM, and BZ performed the experiments. HB, MLB, MX, and BZ analyzed the data. BZ wrote the paper.

Competing interests: The authors have declared that no competing interests exist.

Goodman, 1996). Although neuronal activity is involved in these processes (Catalano and Shatz, 1998;Ruthazer and Cline, 2004), recent evidence suggests that the formation of synapses may be more âhard-wiredâ than previously thought due to specific molecular cues (Jefferis et al., 2001;Clandinin and Zipursky, 2002;Ackley and Jin, 2004). A number of molecules have been identified to play a prominent role in axonal guidance, including semaphorins, ephrins, netrins, neurotrophins, and receptor protein tyrosine phosphatases. Other molecules are more directly involved in synaptogenesis, synaptic growth, or maintenance. These molecules include bone morphogenetic protein (Alberle et al., 2002;Marques et al., 2002;Rawson et al., 2003;McCabe et al., 2003;Keshishian and Kim, 2004), ubiquitin (Oh et al., 1994;DiAntonio et al, 2001;Murphey and Godenschwege, 2002;DiAntonio and Hicke, 2004), cell adhesion molecules (Washbourne et al., 2004), and Wingless signaling components (Packard et al., 2003;Charron and Tessier-Lavigne, 2005).

Flamingo (also known as Starry night) is an atypical cadherin conserved in both structure and function in fruit flies, amphibians, and mammals. Like other cadherins, Flamingo has a number of cadherin repeats and EGF-like motifs in its extracellular domain (Usui et al., 1999;Tepass et al., 2000). Unlike most cadherins, however, Flamingo also possesses seven-transmembrane domains and belongs to the type B G-protein-coupled receptor for cell-cell signaling (Usui et al., 1999;Hill et al., 2001;Harmar, 2001). Flamingo was initially found in *Drosophila* to play a key role in planar cell polarity through the Frizzled-dependent signaling pathway (Usui et al., 1999;Chae et al., 1999;Lu et al., 1999). In the *Drosophila* nervous system, it acts through a yet unidentified signaling pathway to regulate dendritic growth (Gao et al., 2000;Sweeney et al., 2002;Reuter et al., 2003), axonal projection, and target selection (Sweeney et al., 2002;Reuter et al., 2003;Lee et al., 2003; and Senti et al., 2003). Many of these functions are conserved in mammalian orthologs of Flamingo, Celsr (Curtin et al., 2003;Shima et al., 2004;Tissir et al., 2005).

The role of Flamingo in development and function of neuromuscular junctions (NMJs) has not been studied. To this end, we have investigated the larval NMJ of the *flamingo* (*fmi*) mutant. The *Drosophila* NMJ is a well-known model system for studying synaptic formation and growth at the single cell level (Keshishian et al., 1993; Budnik and Gramates, 1999;Hoang and Chiba, 2001). The larval bodywall muscle-synapse is segmented and readily recognized anatomically. Each hemi-segment of a larval bodywall usually contains more than 30 different muscles innervated by â40 motoneurons in stereotypic patterns. Within individual muscles, two to four different synaptic inputs are distinguishable by the morphology of synaptic boutons. In this study, we report that Flamingo plays a major role in synaptic target selection and synaptogenesis, but not in synaptic growth or function. We also find that Flamingo helps prevent age-dependent axonal degeneration and synapse loss. These findings suggest possible roles for Flamingo in synaptic development and neuroprotection.

Results

Flamingo is Expressed in Axons and at Synapses

In a collaborative genetic and functional screen, the Zipursky laboratory and we identified mutant flies defective in both optomotor behavior and electroretinogram (Lee et al., 2003;supplementary Fig. S1A). Further analysis revealed that two mutant lines were allelic to previously identified *fmi* mutations (Usui et al., 1999;Gao et al., 2000;Lee et al., 2003). Flamingo has been shown to be present and well studied in peripheral sensory cells, axons of central nervous system of embryos and larvae (Sweeney et al., 2002), in axons and growth cones of photoreceptors in 3rd instar larvae and mid-pupae (Lee et al., 2003;Senti et al., 2003). However, its presence and roles in the motor system remains unknown. To this end, we first used a monoclonal antibody (Usui et al., 1999) to localize Flamingo in the nervous system of embryos.

Consistent with Sweeney and colleagues (2002), we found that Flamingo was highly expressed in the axons of central nervous system (CNS) within the ventral nerve cord (VNC) and in sensory cells and axons of the peripheral nervous system (PNS) of embryos (see inset in Fig. 1A). When imaged on a different focal plane, Flamingo was clearly detected on the nerve roots existing the VNC and on axonal tracts projecting to bodywall muscles (Fig. 1A & **A1**). These axonal tracts included the intersegmental nerve (ISN) that innervates dorsal muscles, the segmental nerve SNa that innervates ventral-lateral muscles, and the SNb that innervates medial-lateral muscles (Keshishian et al., 1996;Fig. 1A1). Using a polyclonal antibody to the synaptic vesicle protein synaptotagmin I (Mackler et al., 2002), the presynaptic area of the NMJ was readily identified. These results show that synaptotagmin I is highly enriched at the NMJ whereas Flamingo is primarily present on axons.

To examine whether Flamingo is also present at synaptic boutons, we microdissected embryos so that we could directly examine the NMJ. Our results showed that Flamingo was present at a low level in muscle fibers and at a slightly higher level at synaptic boutons and in axons (Fig. 1B & **C**). Importantly, Flamingo was colocalized with synaptotagmin I at NMJs, suggesting that Flamingo is present at presynaptic terminals. As a further support to the observation that Flamingo is localized to axons, we showed that Flamingo and HRP (a neuronal membrane marker) were found on axons in the VNC and axonal projections (Fig. 1D).

fmi Mutants Grow Slowly During 3rd instar Stages and Are Sluggish in Locomotion

Flamingo became undetectable in 2nd and 3rd instar larvae using immunocytochemistry (not shown), suggesting that the protein level in neurons was reduced. This observation may be consistent with an earlier Northern blot analysis showing that RNA levels drop dramatically from embryos to larvae (Chae et al., 1999). However, this may not suggest that Flamingo is all absent, as it is still transiently expressed in larval photoreceptors (Lee et al., 2003;Senti et al., 2003). To further examine Flamingo expression in the CNS (brain lobes plus the VNC) in embryos and developing larvae, we used Western blot to detect protein levels. Our results showed that Flamingo was expressed in embryos and 1st (see 28) and 2nd instar larvae (not shown), and in the CNS and the VNC of 3rd instar larvae (Fig. 2A). Importantly, Flamingo was absent in the CNS of *fmi^{E59}/Df* mutants but could be restored in rescued larvae by neuronal expression of the wild type Fmi (UAS-Fmi) in the mutant background using Elav Gal4 (Fig. 2A).

In the absence of Flamingo, late larval development was delayed. To follow the developmental course of *fmi* mutants, we crossed *fmi^{E59}/CyO krGFP* with *Df(2R)stan^{2}/CyO KrGFP*, a small deficiency that covers the *fmi* locus (Chae et al., 1999). The *fmi^{E59}/Df* mutant larva was identified as GFP-negative larvae. In the wild type control, 91.3 Â 1.9% (n=3) of the 460 fertilized eggs successfully hatched. 98.0 Â 4.7% (n=3) lived to 3rd instar stage. Out of a total of 700 fertilized eggs in the *fmi^{E59}/CyO KrGFP* and *Df/CyO KrGFP* cross, 70.3 Â 2.9% (n=3) of them hatched and became first instar larvae. On average 58.8 Â 2.6% (n=3) of *fmi^{E59}/CyO KrGFP* and *Df/CyO KrGFP* larvae lived to 3rd instar larval stage. This rate is slightly lower than the expected number of 66% (i.e. 2/3 of the progeny). For the *fmi^{E59}/Df* mutant, 7.6 Â 0.9% (n=3) of the first instar larvae lived to 3rd instar larval stage. This rate is significantly below the expected value of 33%, suggesting that most mutant animals die during early development. Nonetheless, the âescapingâ larvae lived to 3rd instar stage and died just prior to or during pupation.

However, we noted that although they reached the early 3rd instar stage at a normal rate, the *fmi* mutant larvae were smaller in body size compared to the wild type instar when they were both 7 days old (Fig. 2B & **C**). These mutant larvae, however, continued to forage in the food and eventually grew to mature 3rd instar in 4-7 more days. Their body size became slightly larger compared to wild type wandering 3rd instars (Fig. 2D). In comparison to the wild type

counterpart, the mutant larvae were sluggish in locomotion either spontaneously or in response to a gentle poking on the head or tail. This is illustrated by a series of sequential still photographs of locomotive positions of the wild type and the *fmi^{E59}/Df* mutant larvae (Fig. 2E). The wild type larva wandered off a penny in 17 seconds and crawled away onto the microscope stage. In contrast, the *fmi* mutant larvae only moved slightly in the original location and never crawled off the penny during the 1 min and 30 sec observation period. The average speed by which larvae moved on the penny was 0.79 Â 0.03 mm/Sec (n=4) for the wild type and 0.14 Â 0.02 mm/Sec (n=5) for the *fmi^{E59}/Df* mutant ($p<0.001$). Hence, the *fmi^{E59}/Df* mutant larvae are defective in locomotion.

fmi Mutations Promote the Formation of Ectopic Synapses

The localization of Flamingo to motor axons and NMJ synapses suggests that it may have other functions in motoneurons and at the NMJ. Defects in axonal projections in *fmi* mutants have been implicated at the embryonic NMJ (Usui et al., 1999) and shown in sensory cells (Sweeney et al., 2002), in the fly visual system (Lee et al., 2003;Senti et al., 2003), and mushroom bodies (Reuter et al., 2003). Additionally, mice deficient in Celsr3 have also been shown to have aberrant and overgrown axons in the brain and spinal cord (Tissir et al., 2005). Consistent with these observations, we noted that one or two segments in 2 out of 15 larvae the SNa nerve reached muscle 12 abnormally from beneath muscle 13 (data not shown). Most muscles, however, appeared to have their normal input. This low rate of axon guidance errors may be a result of corrections known to occur during larval development (Kopczynski et al., 1996). Furthermore, we found that loss of function in one allelic combination (*fmi^{E59}/Df*) slightly increased the number of synaptic boutons per muscle (supplementary Fig. S2). However, other allelic combinations or neuronal overexpression of Flamingo did not have a significant effect on bouton numbers at the NMJ.

Although we did not focus on axon guidance in embryos in this study, we observed another evidence for axonal projection errors in 3rd instar larvae. This is shown by the formation of ectopic synapses formed by an axon erroneously projecting to a muscle that it normally does not innervate. We observed a dramatic increase in the number of ectopic synapses on *fmi* mutant muscles. Most of these ectopic synapses formed on muscles 4, 12, and 13. One type of ectopic synapse is the formation of type I boutons. For example, muscle 12 normally receives synaptic inputs from four types of motoneurons forming type Ib, Is, type II, and type III synaptic boutons (Jia et al., 1993;Atwood et al., 1993). In *fmi* mutants, muscle 12 often received ectopic synapses from axons coming from the transverse nerve or the intersegmental nerve even if its normal synaptic inputs were present. 27.2 Â 5.6% (n=12) and 21.0 Â 3.3% (n=16) of muscle 12 had ectopic type I synapses in *fmi^{E59}/Df* and *fmi^{E59}/fmi^{72}* larvae, respectively, whereas only 1.5 Â1.0% (n=13) of muscle 12 in the *w* control larva received type I input (Fig. 3A, **B, & D**). 12.1 Â 2.6% (n=12) and 14.8 Â 2.5% (n=16) of muscle 13 had ectopic type I synapses in *fmi^{E59}/Df* larvae and in *fmi^{E59}/fmi^{72}* larvae, respectively (Fig. 3C & **E**). All these are significantly higher than that in the control larvae ($p<0.05$). The number of muscles receiving type I ectopic synapses was effectively rescued to near control levels (5.5 Â 2.2%, n=13, $p<0.05$) by neuronal expression of the wild type Flamingo in the *fmi^{E59}/fmi^{72}* mutant background (Fig. 3C-E). However, neuronal expression of the truncated Flamingo only partially rescued the number of muscles with ectopic type I synapses (8.8 Â 3.1%, n=6, $p>0.05$; not shown).

Another type of ectopic synapse is the formation of type II synapses (41, 42, 44; Fig. 3F & **G**). In 73.3 Â 3.3% (n=12) of the cases in *fmi^{E59}/Df* larvae muscle 4 was innervated by type II motoneurons, whereas only 15.4 Â 3.1% (n=13) of muscle 4 normally receives type II innervations in the control larvae. *fmi^{E59}/fmi^{72}* larvae also had significantly more muscles (70.5 Â 3.0%, n=16) innervated by type II motoneurons compared to the control larvae ($p<0.001$). Pan neuronal expression of Flamingo in the *fmi^{E59}/fmi^{72}* mutant background significantly

rescued this defect, reducing the incidence of muscle 4 receiving type II synapses to 27.3 Â 3.6% (n=13, p<0.001). Interestingly, neuronal expression of the truncated Flamingo was slightly less efficacious in reducing the number of type II-innervated muscles to 55.7 Â 6.9% (n=6, p<0.05). The observation of ectopic synapses in *fmi* mutants suggests that Flamingo normally signals the proper target for synapse formation and suppresses abnormal axonal projection.

fmi Mutations Promote the Formation of â*En Passant*â Synapses on Specific Muscles

A role for Flamingo in synaptogenesis was revealed in our analysis of other NMJs in 3rd instar larvae. We found abnormal formation of synapses on a small subset of dorsal muscles. As shown in Figure 4A & **A1**, the ISN nerve traveled towards dorsal muscles 3, 2, and 1 and formed a typical âbeads-on-a-stringâ pattern of synapses extending along the surface of these muscles (Hoang and Chiba, 2001). However, approximately 90% of the synapses found onto muscle 2, and to a lesser extent, onto muscle 3, in fmi^{E59}/Df larvae differed dramatically from the control synapses. On these muscles, synaptic bouton-like varicosities appeared within individual axons along the ISN nerve tract in fmi^{E59}/Df larvae (Fig. 4B-B2). These axons traveled as a bundle (stained with anti-HRP), formed varicosities along the axon when they reached muscles 3 and 2, and then converged as a bundle again before proceeding towards muscle 1. However, synapses onto muscle 1 were not significantly affected (not shown) despite the formation of these axonal varicosities on muscles 2 and 3. These axonal varicosities were typically larger than regular synaptic boutons and were positive for the synaptic vesicle marker synaptotagmin I (Fig. 4) and other vesicle markers (not shown). These varicosities were found randomly at a low rate (â3-5 per larva) throughout all segments; there was no particular preference for one segment. These â*en passant*â varicosities also had presynaptic active zones (marked by the nc82 antibody, Wagh et al., 2005) and postsynaptic receptors (Marrus et al., 2004) and functioned normally in response to nerve stimulation (Fig. 5). These observations indicate that the axonal varicosities are indeed functional synapses. A lack of major effects on synaptic transmission in most muscles was also detected in most other muscle fibers (Fig. S1B-E). These results suggest that Flamingo does not play a major role in synaptic function.

Further analysis of 1st instar larvae showed that *en passant* synapses formed early during development (see supplementary Fig. S3). The number of *en passant* synapses per larva was similar in 1st (n=5) and 3rd instar (n=7) fmi^{E59}/Df larvae (p>0.05), but it is slightly higher in fmi^{E59}/fmi^{72} mutants (n=5, p<0.01). Neuronal expression of the wild type Flamingo in the fmi^{E59}/fmi^{72} mutant background significantly suppressed the formation these *en passant* varicosities and restored most of the NMJ to normal âbeads-on-a-stringâ morphology seen in the wild type (n=13, p<0.01) (Fig. S3E). These observations suggest that neuronal Flamingo normally prevents the formation of these ectopic *en passant* synapses.

Synaptic Bouton-like Varicosities Also Form within Axons Along the Segmental Nerve in the Absence of Target Cells

Our strongest support for Flamingo's role in synaptogenesis is the observation that synaptic bouton-like varicosities form along axons within segmental nerves. In *w* control larvae, the segmental nerve was usually devoid of accumulation of synaptic proteins, such as synaptic vesicle proteins (CSP, Zinsmaier et al., 1994; n-Syb, Wu et al., 1999; and Syt I), the endocytotic and trafficking proteins (clathrin heavy chain, LAP, Zhang et al., 1998; and DAP160; Roos and Kelly, 1999), the active zone (nc82), and the peri-active zone protein Highwire (Hiw; Wan et al., 2000). Examples of axons in the control larvae stained for the vesicle protein Syt I in 1st instar larvae and the endocytotic protein DAP160 in 3rd instar larvae are shown in Figure S3B and Figure 6A, respectively. In contrast to the control animal, *fmi* mutants accumulated these proteins in a pattern similar to NMJ synaptic boutons along the segmental nerve (Fig. S3D & Fig. 6B). These varicosities could be shown on axons labeled with the antibody 22C10

to the MAP1B protein Futsch (Roos et al., 2000;Hummel et al., 2000) and examined at high magnification (Fig. 6B). In 1st instar mutant larvae, 6.4 Â 0.24 (n=5) of the segmental nerves exhibited axonal varicosities (Fig. S3F). The number of segmental nerves found to have such axonal varicosities was 6.58 Â 0.72 (n= 12 larvae) in fmi^{E59}/Df and 6.75 Â 0.85 (n=4) in fmi^{E59}/fmi^{72} 3rd instar larvae. In rescued fmi^{E59}/fmi^{72} 3rd instar larvae, this number was significantly reduced to 1.00 Â 0.32 (n=13; $p<0.001$). The varicosity occurred randomly along the segmental nerve, but appeared to present more frequently in the anterior nerve after exiting the VNC.

To investigate whether these axonal varicosities contained presynaptic specializations similar to those found at regular NMJs, we used a battery of antibodies against various presynaptic terminal proteins to stain the mutant segmental nerve. Indeed, CSP, n-Syb, Syt I, and the *Drosophila* vesicular glutamate transporter (VGluT, Daniels et al., 2004) were respectively found to colocalize within these varicosities (Fig. 6C-F). The most surprising finding is that these active zones were well organized in a pattern similar to those found at presynaptic terminals at NMJs. These observations suggest that these axonal varicosities are likely to have presynaptic structures similar to those found in the nerve terminal. This defect was also observed in the fmi^{E59}/fmi^{72} mutant (Fig. 6G) and was rescued by expression of the wild type Flamingo in postmitotic neurons (Fig. 6H). We have attempted but failed to identify these varicosities using electron microscopy. Unlike the *en passant* synapses found on muscles 2 and 3, however, these axonal varicosities did not have postsynaptic glutamate receptors (data not shown). It should be noted that these axonal varicosities differ from protein aggregates caused by traffic jam of axonal transport, such as in mutations affecting kinesin or dynein motor-dependent axonal transport (Kurd and Saxton, 1996; Martin et al., 1999; data not shown).

The *fmi* Mutant Larva Displays An Age-dependent Synapse Loss at the NMJ

Electrophysiological recordings from larval bodywall muscles showed that the majority (>90%) of muscles responded to nerve stimulation normally (see Fig. S1B-E; Fig. 8A). However, a small subset (<10%) of muscles produced dramatically small EJPs or no EJP at all (Fig. 7A). Because the resting potential of these muscles was relatively normal, these unusually small EJPs or lack of EJPs suggested muscle denervation in the mutant. To test this hypothesis, we examined bodywall muscle NMJs in 3rd instar larvae. In control larvae, muscles 6/7, 12, and 13 all had their normal synapses (n=12 larvae. Fig. 7B). In fmi^{E59}/Df larvae 15.5 Â 3.3% (n=12 larvae) of muscle 12 and 8.7 Â 1.2% (n=16 larvae) of muscle 13 had completely lost their NMJs (Fig. 7C-E). In fmi^{E59}/fmi^{72} larvae, 8.6 Â 2.6% (n=12) of muscle 12 and 4.7 Â 1.8% (n=16) of muscle13 did not have synaptic innervation at all. Approximately 7% and 2% of muscles 6/7 were without synaptic innervation in fmi^{E59}/Df and fmi^{E59}/fmi^{72} larvae, respectively. All these defects are significantly different from the control larva ($p<0.05$ for muscles 6/7, and $p<0.0001$ for muscles 12 and 13). The defects in muscles 13 and 6/7 were completely rescued by neuronal expression of wild type Flamingo ($p<0.05$), but were only partially rescued in muscle 12 ($p>0.05$) (Fig. 7D & **E**). None of these defects was rescued by neuronal expression of the truncated Flamingo in the fmi^{E59}/fmi^{72} mutant background (Fig. 7D & **E**).

The lack of muscle innervation in 3rd instar mutant larvae could result from one or a combination of three factors: defects in neurogenesis, errors in axon guidance or an age-dependent loss of motor axons during development. Should either of the first two possibilities be responsible for the loss of synapses, one would expect that a similar fraction of muscles would be without synaptic innervation in younger animals. Additionally, potential corrections of axonal projection errors during larval development could further reduce the number of muscles losing synapses in 3rd instar larvae. One would then expect to find more dennervated

muscles in younger larvae. To test this possibility, we examined synaptic innervation in 1st and 2nd instar *fmi*^{E59}*/Df* mutant larvae. We found that significantly fewer muscles 12 and 6/7 lacked synapses in 2nd instars compared with the 3rd instar larvae (n=9) (Fig. 7F & **G**). On average, 4.5 Â 1.8% of muscle 12, whereas 1.1 Â 1.1% of muscles 6/7 and of muscle 13 did not have synapses in 2nd instar larvae (n=9). All muscles in *w* control larvae at the same developmental stage also had normal synaptic innervation (n=7). With the exception of muscle 12, synapse loss in these muscles of the 2nd instar mutants was not significantly different from that in the control larvae ($p>0.05$). However, there was a significant increase in the fraction of muscles losing synapses from 2nd to 3rd instar larvae ($p<0.05$ for muscles 12 and 6/7 and $p<0.0001$ for muscle 13). None of the muscles in 1st instar mutant larvae lost synaptic innervation (Fig. 7F-G). These results suggest that NMJs in the *fmi* mutant form initially in early developing embryos and remain in 1st instar larvae and that synapse loss begins during 2nd instar and progresses during 3rd instar larval development.

The *fmi* Mutant Larva Undergoes Dramatic Axonal Degeneration in Segmental Nerves

The loss of NMJs in developing larvae suggests that motoneurons or axons undergo degeneration in *fmi* mutants. To examine this possibility, we sectioned the segmental nerve from the *fmi*^{E59}*/Df* mutant and *w* control 3rd instar larvae for electron microscopy. We examined a number of segmental nerves from one control larva and two mutant larvae. Representative electron micrographs and a summary of the results are shown in **Figures** 8 **and** 9, respectively. Our electron micrographs revealed several differences in the size and integrity of the segmental nerve, which contains motor axons as well sensory axons. First, the average diameter and total cross-sectional area of the segmental nerve was smaller in the mutant compared with the control larvae (Fig. 8A & **B**, and Fig. 9A). The average cross-sectional area of the segmental nerve in the *fmi*^{E59}*/Df* larvae (2.2 Â 0.14 Ã 10^7 nm^2, n=13 nerves) was significantly smaller than that of the control larvae (2.9 Â 0.22 Ã 10^7 nm^2, n=9; $p<0.01$).

Second, the wild type nerve was tightly packed with axons and glial processes (Fig. 8A-A2). In contrast, the mutant nerve appeared to have more gaps, which were likely left behind by axons that had undergone degeneration (Fig. 8B-B2). Signs of typical degenerating axons, such a breakup of axonal membranes and a loss of microtubules, are clearly notable (Fig. 8B1). In support of this notion, the average number of axons per segmental nerve was significantly reduced to 30.6 Â 1.8 (n=13) in the *fmi*^{E59}*/Df* larva from 81.7 Â 1.6 (n=9) in the control larva ($p<0.01$). This 63% reduction in the number of axons within a segmental nerve is statistically significant ($p<0.01$) (Fig. 8B), even after it is normalized to the total area of the segmental nerve (Fig. 8C). The average cross-sectional area of the remaining axons was similar in the mutant (57743.4 Â 2934.8 nm^2, n=13) and the control larvae (56358.2 Â 4048.6 nm^2, n=9).

Third, the peripheral glial sheath surrounding the segmental nerve was thicker in the mutant (179.3 Â 5.6 nm, n=13) compared with that in the control larvae (140.2 Â 29.0 nm, n=9; $p<0.01$) (Fig. 8A2 & **B2**, & Fig. 9D). Finally, the average area of glial processes was also significantly reduced in the segmental nerve of the *fmi* mutant. The ratio of glial area to the nerve area was reduced from 0.49 Â 0.03 (N=13) in the *w* control larvae to 0.33 Â 0.02 (N=9) in the *fmi* mutants ($p<0.01$). Together with the progressive loss of both muscle innervation and synaptic responses observed in the *fmi* mutant, these ultrastructural results indicate that motor axons as well as sensory axons degenerate during larval development. These defects may explain why *fmi* mutant larvae were sluggish, especially at late 3rd instar stages and usually died in the food prior to or during pupation.

The Number of Sensory Cells Appears Normal in the *fmi* Mutant Larvae

The number of missing axons is far greater than the number of muscles that have lost NMJs, suggesting that the majority of axons undergoing degeneration are sensory axons, which are

also components of the segmental nerve. We then decided to examine whether there was a corresponding loss or degeneration of sensory cells in the PNS (see supplementary Fig. S4). Our results showed that the average number of sensory cells (multidendritic neurons and external sensory cells) in the dorsal cluster was 10.97 Â 0.36 (n=11 larvae, N=59 segments) and 9.89 Â 0.33 (n=21, N=55) in the wild type and the *fmi* mutant larvae, respectively. This difference is quite small, however, statistically significant (p=0.046). Given this rather minor difference in the sensory cell number, we also examined a group of multidendritic neurons, vdaA-D and vbd, in the ventral cluster. The average number of these multidendritic cells was 4.85 Â 0.09 (n=13, N=47) in the wild type and 4.91 Â 0.09 (n=16, N=66) in the *fmi* mutant (p=0.62). The total average cell number from these two cluster was not significant different between the wild type (7.65 Â 0.66, n=24) and fmi^{E59}/Df larvae (7.74 Â 0.45, n=37) (p=0.91), suggesting that axons degenerate without an apparent death of neurons during larval development.

Neuronal Expression of the Wild Type Flamingo Rescues Axonal Degeneration and Larval Lethality

One may be concerned that the loss of synapses could result from the slow development of *fmi* mutant larvae or their death prior to pupation. However, we deem this very unlikely because synapse loss already begins in the lively 2nd instar larvae. To ensure that the defects we have observed here in the *fmi* mutant are specifically caused by the loss of function of Flamingo, we have carefully performed rescuing experiments by introducing the wild type *fmi* gene into the mutant background using the pan neuronal driver Elav Gal4 and UAS-Fmi. We have earlier shown that neuronal expression of the wild type Flamingo is sufficient to rescue partially or fully the defects in formation of ectopic synapses, *en passant* synapses, axonal varicosities, and synapse denervation (**Figs.** 2-4, 6-8).

We next examined the segmental nerve in rescued larvae using electron microscopy and showed that axonal de generation could also be rescued (Fig. 8C & Fig. 9). In rescued larvae, the segmental nerve had a larger diameter compared to both the wild type and the *fmi* mutant. The average nerve area was 5.50 Â 1.11 Ã10^{7} nm^{2} (n=4 nerves), which is significantly larger than that in the *fmi* mutant (p<0.001) and the wild type (p<0.01) (Fig. 9A). A small number of axons (approximately 2-3 per segmental nerve) had large vacuoles (Fig. 8C1), suggesting that they were partially rescued axons or they underwent degeneration. Nonetheless, the overall rescue was remarkably successful. Similar to the wild type, the segmental nerve in the rescued larvae was more tightly packed with a high number of axons and glial processes (Fig. 8C-C2). The average number of axons was 113.00 Â 17.90 (n=4), which is slightly larger compared to the wild type (p<0.05) but significantly higher compared to the *fmi* mutant (p<0.001) (Fig. 9B). When normalized to the area of the segmental nerve, the number of axons was 2.07 Â 0.18 Ã$10^{â6}$ per nm^{2}. This is similar to those found in the wild type (p>0.05), but clearly higher compared to the fmi mutant (p<0.001, Fig. 9C). Finally, the thickness of the peripheral glial sheath surrounding the segmental nerve was also rescued to the wild type level (122.29 Â 9.0 nm, n=4; Fig. 9D). These results strongly suggest that *fmi* loss of function specifically causes the axonal degeneration observed in the *fmi* mutant and that neuronal expression of Flamingo is sufficient to rescue axon degeneration.

Finally, we observed tha neuronal expression of Flamingo also rescued larval lethality and resulted in viable adult flies. In 14 separate crosses, we obtained 29.14 Â 2.32 viable F1 rescued adult flies per cross, which represents 73.62 Â 3.35% of the expected number of rescued flies. These rescued flies had disoriented bristles, similar to those shown in clonal analysis (Usui et al., 1999;Chae et al., 1999), and displayed minor behavioral abnormalities (not shown). Hence, neuronal Flamingo is both necessary and sufficient for adult viability.

Discussion

In the present study, we have examined the role of Flamingo in formation, function, and maintenance of NMJs and in axonal health in the *Drosophila* larva. The major findings are that Flamingo regulates synaptic target selection and synaptogenesis and maintains axonal health. We also show that these functions are mediated by the presence of Flamingo only in postmitotic neurons.

Flamingo is Crucial for both Target Selection and Synaptogenesis

Flamingo appears to be important for both target selection and synaptogenesis depending on tissue types. In muscles 4, 12 and 13, there is an increase in ectopic type I and II synapses in *fmi* mutants. The presence of exuberant ectopic synapses could reflect efforts by neurons to compensate for the loss of synapses to enhance glutamatergic synaptic transmission. However, we do not favor the idea that formation of ectopic synapses is a result of developmental compensation because 1) ectopic type I boutons are not always found in dennervated muscles; and 2) octopamine, which is the major neurotransmitter in type II synapses (Monastirioti et al., 1995), inhibits glutamate-mediated synaptic potentials instead of enhancing them (Nishikawa and Kidokoro, 1999). Alternatively, these ectopic synapses might result from a defect in either synaptic targeting or nerve sprouting. Consistent with this idea, we note the ectopic synapse is reminiscent of aberrant axonal projections in the visual system (Lee et al., 2003;Senti et al., 2003) and the mushroom body in the *fmi* mutant (Reuter et al., 2003) and in the brain and spinal cord of Celsr3-deficient mice (Tissir et al., 2005). Hence, Flamingo likely also regulates both synaptic target selection and axonal projection at the NMJ.

Our observations of axonal varicosities and *en passant* synapses in the *fmi* mutant also suggest that Flamingo plays a role in regulating synaptogenesis. In the absence of Flamingo, synaptic bouton-like varicosities are found along axons within the segmental nerve. The axonal varicosity on the segmental nerve contains proteins for synaptic vesicles, endocytosis, peri-active zones, and active zones. Notably, the organization and size of active zones are strikingly similar to those found in motor nerve terminals at the NMJ, suggesting that these varicosities are potentially true presynaptic structures even now there are no glutamate receptors. The axons within the segmental nerve are wrapped with glial sheath, loosely float inside the larva, and do not contact muscle fibers. Hence, the accumulation of presynaptic varicosities on axons within the segmental nerve could represent an effort to form synapses in the absence of the normal target (i.e. muscles). If indeed these axonal varicosities were synapses without a target, this would be a synaptogenesis defect. On the other hand, if these axonal varicosities were axon-axon synapses, the defect would be target selection. Our data do not allow us to distinguish these two possibilities.

While it is difficult to ascertain the nature of these axonal varicosities, the *en passant* synapses found on muscles 2 and 3 in *fmi* mutants are clearly functional synapses. The formation of such synapses on these dorsal muscles may serve to replace their normal pattern of boutons spreading along the muscle surface as âbeads-on-a-stringâ. Interestingly, these defects on dorsal muscles share some similarities with those found in the eye (Lee et al., 2003;Senti et al., 2003). In both cases, axons are able to reach the general target area. However, these axons fail to form normal synapses in both the retina and these dorsal muscles. One perplexing aspect of our observations is that the NMJs on other muscles, including the downstream muscle 1, appear normal. At present, we do not know the special properties that make muscles 2 and 3 targets of synaptogenesis defective. We speculate that specific ligands or cell adhesion molecules on muscles 2 and 3 may be involved in Flamingo signaling during synaptogenesis. While remaining an interesting question for future studies, we realize greater efforts are needed to pinpoint such muscle-specific ligands or cell adhesion molecules. Nonetheless, our results are

consistent with the possibility that Flamingo plays a role in synaptogenesis and in suppression of *en passant* synapses.

How might Flamingo regulate synaptogenesis? Both the axonal varicosities and *en passant* synapses are novel and have not been reported before in other *Drosophila* mutants. *En passant* synapses are a normal type of synapse found in a variety of animals, including *C. elegans* (Ackley and Jin, 2004), *Drosophila* (Egger et al., 1997), *Aplysia* (Hatada et al., 1999), the leech (Tai and Zipser, 1999), and mammals (Dailey et al., 1994). In *Drosophila*, *en passant* synapses have been described in the giant fiber pathway (Egger et al., 1997), but have not been found at larval NMJs. The formation of *en passant* synapses has been well studied in developing neurons of the leech, *Aplysia*, and mammals. Although the precise mechanism of synaptogenesis has yet to be resolved, it is currently believed that local regulation of cell adhesion molecules is required for the initial formation of presynaptic specializations (Goda and Davis, 2003;Washbourne et al., 2004). Recent studies also suggest that molecules needed to form presynaptic specializations are pre-packed in vesicles and travel along the axon (Ahmari et al., 2000;Shapira et al., 2003). Such pre-packed molecules make it more convenient for an axon to form synapses, including *en passant* synapses along its tract. Because the formation of such *en passant* synapses is normally suppressed along the *Drosophila* larval segmental nerve, we suggest that Flamingo exerts an inhibitory effect on ectopic synaptogenesis by either signaling through its G-protein-coupled receptor or its cell adhesion repeats. At present, we do not know whether Flamingo regulates the trafficking of pre-packed synaptic cargos or the local concentration of cell adhesion molecules along the axon.

Flamingo Helps Prevent Axonal Degeneration and Synapse Loss

Synapse loss and axonal degeneration are recognized as the initial morphological changes of the nervous system in a number of neurological disorders (Raff et al., 2002âLuo and O'leary, 2005). The morphological changes of axons and synapse loss in *fmi* mutants are reminiscent of the hallmarks of neurodegenerative diseases. In the *fmi* mutant, the loss of synapse appears to be progressive and age-dependent. While the NMJ is normal in 1st instar larvae, it begins to degenerate in the 2nd instar stage and becomes more pronounced by the late 3rd instar stage. Since most NMJs are intact, we suggest that the loss of synapses is likely a consequence of axonal degeneration. While the majority of axonal loss is expected to occur in sensory cells, the number of sensory cells remains unaffected in the *fmi* mutant, implying that the mutant larvae undergo axonal degeneration without the cell death, at least in late larval development. This might be similar to the early phase of Wallerian degeneration (Luo and O'leary, 2005). As with the synaptogenesis defects, neuronal expression of Flamingo is sufficient to rescue axonal degeneration and larval lethality. Interestingly, there are more axons per segmental nerve in rescued larvae, suggesting that Flamingo may even protect axons programmed to die during larval development. This clearly requires further investigations in the future. Nonetheless, the successful rescue of axonal and synaptic degeneration as well larval lethality provides good evidence that Flamingo indeed has a neuroprotective role.

It should be noted that neurodegeneration is not limited to the larvae nervous system or flies. In mushroom bodies of the *fmi* mutant, Reuter and colleagues (2003) have observed a significant reduction in the number of cell bodies, suggesting that neuronal death or defects in neurogenesis may have occurred during or after metamorphosis. Furthermore, the observation of axonal swelling in cortices suggests that axonal degeneration may also occur in Celsr3-deficient mice (Tissir et al., 2005). Hence, Flamingo/Celsr may have a conserved function in preventing axonal and synaptic degeneration in fruit flies and mammals. Such a neuroprotective function for Flamingo is also shared by another atypical cadherin family in mammals, which have also been shown to be critically required for the survival of spinal motoneurons (Wang et al., 2002) and for synaptogenesis (Weiner et al., 2005). Therefore,

atypical cadherins have emerged as a unique class of molecules important for multiple neuronal functions, including axonal growth and targeting, synapse formation, maintenance of the health of axons and synapses.

Maintaining axonal health does not necessarily represent a distinct function for Flamingo from those used in synaptogenesis. Homophilic cell adhesion mediated by Flamingo is proposed to determine planar cell polarity, based on the observation that Flamingo self aggregates *in vitro* (Usui et al., 1999). A similar mechanism might also be employed by axons to prevent axon degeneration as well as ectopic and *en passant* synapse formation. This may explain why neuronal expression of Flamingo alone is sufficient to fully rescue most of the mutant phenotypes. However, heterophilic interaction with other CAMs among axons could equally explain our rescue results. Additionally, we have shown that neuronal expression of Flamingo lacking the cadherin domain could partially suppress the overgrowth of type II boutons in the mutant background. This result cannot be explained by either homo- or hetero-philic interaction, as the muscle cells do not have Flamingo in *fmi* mutants and the truncated Flamingo do not have the cell adhesion motif. Loss of function in *flamingo* is known to cause the overexpansion of the dendritic field at the dorsal midline between homologous multidendritic cells (Gao et al., 2000). Such defects can be partially rescued by expression of the wild type Flamingo in multidendritic neurons while the rest of the animal is still deficient in Flamingo. Assuming that homophilic interaction between multidendritic neurons indeed inhibits dendritic overexpansion, one would expect that overexpression of Flamingo in MD cells would reduce dendritic field or at least have no effect on dendritic development. This is clearly not the case. In the same study, Gao and colleagues (2000) showed that overexpression of Flamingo in single multidendritic neurons resulted in overexpansion of dendritic territories. These results suggest that the level of Flamingo in multidendritic neurons is important for its function but do not rule out the possibility that Flamingo could interact with other ligands. Hence, further studies are needed to better understand the basic biology of Flamingo in the nervous system as well as mechanisms of neurodegeneration.

Experimental Methods

Fly strains and genetics

Flies were reared on standard cornmeal-based food at 22ÂC. The following flies were used: fmi^{E59}, UAS-Fmi, UAS-ÎEx (28), $Df(2R)stan^{2}$ (Usui et al., 1999), fmi^{72} (34), *elav-Gal4* (DiAntonio et al., 2001), fmi^{1071} and fmi^{1127} (Lee et al., 2003). *fmi* mutant alleles and the deficiency line were balanced with CyO KrGFP allowing easy selection of GFP-negative *fmi* mutant larvae (Gao et al., 2000). All fly lines were kept in *w* background, and hence *w* was used as the control fly. Mosaic flies in which the photoreceptor cells are homozygous *fmi* mutants whereas the rest of the body is heterozygous for *fmi* were generated by crossing eyFLP; FRT 42 *fmi* /CyO with EGUF; FRT 42 CL HID (Stowers and Schwarz, 1999). To rescue the *fmi* mutant, fmi^{E59}, Elav Gal4/CyO-TM6B, Tb flies were crossed to fmi^{72}, UAS-Fmi/CyO-TM6B, Tb lines. Non-tubby F1 flies were examined as rescued mutant flies.

Biochemistry

Six dissected CNS (brain + VNC) and 12 dissected ventral nerve cords from wild type 3rd instar larvae, and 6 dissected CNS from fmi^{E59}/Df larvae were ground in 70 Îl ice-cold sample buffers. Four dissected CNS from rescued *fmi* mutant larvae were used to prepare for protein extracts in 40 Îl sample buffers. After a brief high-speed centrifugation, 20 Îl of the supernatant was loaded on 5% SDS gel. After electrophoresis and blotting, the nitrocellulose membrane was incubated overnight with a monoclonal antibody to Flamingo (#74,1:10 dilution) at 4 ÂC. The blot was detected for protein levels after incubation with a mouse anti-HRP secondary antibody using the standard ECL method (Amersham Biosciences). Because of the large

molecular weight of Flamingo (â300 Kd; 28), molecules such as tubulin at a low molecular weight ran off the gel. Hence, we loaded equal volumes of the samples to a duplicate gel, ran for a short time, and probed the blot with a tubulin antibody (Sigma) (Fig. 2A). As instructed by Tadashi Uemura (http://www.uiowa.edu/âdshbwww/flamingo.html), the dissection was conducted in HL-3 saline containing 0.8 mM calcium to ensure the stability of Flamingo. The dissected brain and ventral nerve cord in 3rd instar larvae were devoid of the attached imaginal discs and fat tissues to ensure that protein extracts came from the central nervous system.

Immunocytochemistry and Microscopy

Wandering 3rd instar larvae were dissected in calcium-free HL-3 saline and fixed in Bouin's fixative or 4% paraformaldehyde. Following one hour incubation with a blocker solution (2-5% bovine serum albumin, 0.2% Tween-20 in PBS, PBT), the preparation was stained overnight at 4 ÂC using primary antisera, followed by one hour washes with PBT and 1-2 hours incubation with secondary antibodies at room temperature, and visualized using a Nikon fluorescence microscope. The following primary antibodies were used: rat anti-Syb (1:300, Wu et al., 1999), mAb anti-CSP (ab49, 1:20, Zinsmaier et al., 1994), rabbit anti-Syt (1:300, Mackler et al., 2002), mAb anti-Futsch (22C10, 1:100, Developmental Studies Hybridoma Bank), mAb anti-Hiw (6H4, 1:3, Wan et al., 2000), rabbit anti-DAP 160 (1:300, Roos and Kelly, 1999), mAb nc82 (1:20; Wagh et al., 2005), a polyclonal antibody to clathrin heavy chain (1:50) and to LAP (1:200, Zhang et al., 1998), a polyclonal antibody to glutamate receptor III (Marrus et al., 2004), a polyclonal antibody to the *Drosophila* vesicular glutamate transporter (VGluT, 1:500, Daniels et al., 2004), and a polyclonal antibody to HRP (Jan and Jan, 1982). Fluorescence-conjugated secondary antibodies were used 1:100 (Jackson Immunology Labs). Confocal images were acquired using a Leica DMIRE2 or SP2 AOBS microscope with a 63X oil objective microscope. All images were processed using Photoshop and ImageJ 1.29x (NIH). Quantification of synaptic bouton number and muscle size was performed by using a 40X and 4X Nikon objectives on a Nikon microscope, respectively.

The percentage of muscles lacking NMJ synapses was calculated by dividing the number of a specific muscle (e.g. muscle 12) that lost synapses by the total number of the muscle in each larva. For example, 3 out 10 muscles that lost synapses resulted in 30%. The final average percentage loss of synapses for a specific muscle was obtained from at least 7 different animals. Using a similar approach, we determined the percentage of muscles receiving ectopic synapses.

To identify sensory cells in 3rd instar larvae, dissected larvae were fixed in 4% paraformalhyde at room temperature for 1 hr or in Bouin's fixative for 20-30 min and stained with HRP and/or 22C10 antibodies. Dorsal and ventral clusters of multidendritic cells were identified according to their embryonic locations. Images presented in Figure 10 A and B were taken by a Zeiss confocal equipped with the Pascal software.

Electrophysiology

Electrophysiological recordings of synaptic potentials were performed on bodywall muscle 4 in abdominal segment 3 and 4 of third instar larval neuromuscular junction preparation (Jan and Jan, 1976). The larva was bathed in HL-3 solution (Stewart et al., 1994) containing 1 mM calcium (Ca^{2+}) for measuring evoked synaptic potentials and 0.1 mM Ca^{2+} and 1 ÎM tetrodotoxin for recording spontaneous synaptic potentials (Zhang et al., 1998;Bao et al., 2005). To preserve dorsal muscles for intracellular recordings, the dissection method was slightly modified. Instead of incisions usually made along the dorsal midline, we incised the bodywall at positions slightly off the midline such that dorsal muscles on one hemisegment were intact. Additional care was taken to avoid overstretching the preparation laterally, as axons to dorsal muscles tended to break easily.

Intracellular recordings were achieved using sharp microelectrodes (18-25 MÎ, filled with 3M KCl). The excitatory junction potential (EJP) was evoked by stimulating the innervating segmental nerve at 0.2 Hz with a suction electrode. At least five different larvae from each genotype were used for each electrophysiological experiment. The input resistance of muscles was routinely monitored and muscles with an input resistance below 5 MÎ in control larvae were not used. Recordings were performed using an Axoclamp 2B amplifier in current clamp mode. The signal was low-pass filtered at 5 kHz, digitized through a Digidata 1322A acquisition system (Axon Instruments) and stored in a Dell personal computer using Clampex 8.2 software (Axon Instruments). The average EJP amplitude was calculated by averaging 5-10 single EJPs with Clampfit 8.2 (Axon Instruments). The Mini Analysis program (Synaptosoft Inc.) was used to measure the amplitude of individual miniature EJPs (mEJPs or minis). mEJPs with a slow rise time arising from neighboring electrically coupled muscle cells were excluded from analysis (Zhang et al., 1998). The unpaired Student's test was used for the data statistics using Origin software (OriginLab). In addition, the Kolmogorov-Smimov test was administrated when comparing mini size between preparations using Mini Analysis Program. The final figures were generated and processed by using Origin and Photoshop (Adobe).

For electroretinogram (ERG) recordings, a reference electrode was placed inside the abdomen and a recording electrode (filled with 3 M KCl) inserted just below the surface of the compound eye. The fly was kept in the dark and then exposed to a beam of bright light for â2 seconds. ERGs were recorded and analyzed using similar equipment and methods described for larval electrophysiology.

Electron microscopy and quantification

Following initial fixation in Bouin', the specimens were washed in cacodylate buffer and fixed again in 1% osmium tetroxide in 0.1M cacodylate buffer for 1 hour, followed by 1 hour in 2% uranyl acetate in double distilled water. The specimens were buffer-rinsed and then dehydrated in a series of ethanol solutions of increasing concentration for 30 minutes each. Subsequently the specimens were incubated in propylene oxide for two 30-minute intervals followed by a one-hour incubation in a 50:50 mixture of propylene oxide and Embed-812 (Electron Microscopy Sciences, Hatfield, PA). Specimens were then placed on an open rotator overnight in 100% Embed-812 (medium hardness). The following day, specimens were placed in fresh epon in a coffin mold and cured at 60C for 14 hours. Ultrathin sliver-gray sections were cut on an ultramicrotome (Leica Ultracut UCT) using a diamond knife (Diatome). Sections were counterstained with 1% uranyl acetate (aqueous) and Reynold's lead citrate and examined and photographed using a Philips EM208 transmission electron microscope (FEI Company, Hillsboro, OR) at 80kv. Images at 1 Mb in size were collected with an AMT Advantage HT (Danvers, MA) camera. All photographs were taken at a magnification of 11000.

Digital images were adjusted for brightness, contrast, and gamma in Adobe Photoshop 7.0 (San Jose, CA). Nerve sheath thickness was calculated in Adobe Photoshop using a pixel to nanometer ratio derived from the image scale bar. All other parameters (object numbers and pixel areas) were measured using thresholded images in Metamorph 6.1 (Sunnyvale, CA). Glia and axons (identified by the presence of microtubules) were selected in Adobe Photoshop and marked for further measurement in Metamorph's âIntegrated Morphometry Analysisâ. Data was exported to Microsoft Excel (Redmond, WA) for statistical analysis.

Supplementary Material

Refer to Web version on PubMed Central for supplementary material.

Acknowledgements

We thank Chi-Hon Lee, Roger Lee, Thomas Clandinin, and Larry Zipursky for collaborating with us on a screen for defects in the âonâ and âoffâ transients in the fly lines (including *fmi* alleles) defective in optomotor and phototaxic behavior. We thank our colleagues (referenced in the text) for providing antibodies and fly lines. We thank Ruth Buskirk and NSF (DBI 0139881) for sponsoring S.M.H. as a REU Fellow in Molecular Biology at the University of Texas at Austin, John Sisson for the use of his confocal microscope, Angela Bardo at UT's core microscopic facility for assistance in confocal imaging, Kristen Frye (at CSHL) and Carl Zeiss Inc. for the use of confocal microscope, Wesley Thompson for the use of his microscope, Feng-Biao Gao for help with the identification of PNS neurons. We thank Wesley Thompson, Veronica Martinez, and Chris Spaeth for constructive comments on the manuscript. This research was supported by a start-up fund from the UT-Austin (to B.Z.), in part by an NSF CAREER Award (IBN-0093170, to B.Z.) and in part by an NIH/NIEHS grant (ES014441, to B.Z.), by a Undergraduate Research Fellowship (to R. W. D.), in part by an NIH National Research Service Award (NRSA, DA016807-01, to M.L.B.), and in part by a grant from the National Institute on Alcohol Abuse and Alcoholism (AA13497-04-INIA to A.A.A).

References

Aberle H, Haghighi AP, Fetter RD, McCabe BD, Magalhaes TR, Goodman CS. wishful thinking encodes a BMP type II receptor that regulates synaptic growth in Drosophila. Neuron 2002;33:545â558. [PubMed: 11856529]

Ackley BD, Jin Y. Genetic analysis of synaptic target recognition and assembly. Trends Neurosci 2004;27:540â547. [PubMed: 15331236]

Ahmari SE, Buchanan J, Smith SJ. Assembly of presynaptic active zones from cytoplasmic transport packets. Nat Neurosci 2000;3:445â451. [PubMed: 10769383]

Atwood HL, Govind CK, Wu CF. Differential ultrastructure of synaptic terminals on ventral longitudinal abdominal muscles in Drosophila larvae. J Neurobiol 1993;24:1008â1024. [PubMed: 8409966]

Bao H, Daniels RW, Macleod GT, Charlton MP, Atwood HL, Zhang B. AP180 maintains the distribution of synaptic and vesicle proteins in the nerve terminal and indirectly regulates the efficacy of Ca^{2+}-triggered exocytosis. J Neurophysiol 2005;94:1888â1903. [PubMed: 15888532]

Budnik, V.; Gramates, LS. Neuromuscular Junctions in Drosophila. Academic Press; San Diego, USA: 1999.

Catalano SM, Shatz CJ. Activity-dependent cortical target selection by thalamic axons. Science 1998;281:559â562. [PubMed: 9677198]

Chae J, Kim MJ, Goo JH, Collier S, Gubb D, Charlton J, Adler PN, Park WJ. The Drosophila tissue polarity gene starry night encodes a member of the protocadherin family. Development 1999;126:5421â5429. [PubMed: 10556066]

Charron F, Tessier-Lavigne M. Novel brain wiring functions for classical morphogens: a role as graded positional cues in axon guidance. Development 2005;132:2251â2262. [PubMed: 15857918]

Clandinin TR, Zipursky SL. Making connections in the fly visual system. Neuron 2002;35:827â841. [PubMed: 12372279]

Curtin JA, Quint E, Tsipouri V, Arkell RM, Cattanach B, Copp AJ, Henderson DJ, Spurr N, Stanier P, Fisher EM, Nolan PM, Steel KP, Brown SD, Gray IC, Murdoch JN. Mutation of Celsr1 disrupts planar polarity of inner ear hair cells and causes severe neural tube defects in the mouse. Curr Biol 2003;13:1129â1133. [PubMed: 12842012]

Dailey ME, Buchanan J, Bergles DE, Smith SJ. Mossy fiber growth and synaptogenesis in rat hippocampal slices in vitro. J Neurosci 1994;14:1060â1078. [PubMed: 8120613]

Daniels RW, Collins CA, Gelfand MV, Dant J, Brooks ES, Krantz DE, DiAntonio A. Increased expression of the Drosophila vesicular glutamate transporter leads to excess glutamate release and a compensatory decrease in quantal content. J Neurosci 2004;24:10466â10474. [PubMed: 15548661]

DiAntonio A, Haghighi AP, Portman SL, Lee JD, Amaranto AM, Goodman CS. Ubiquitination-dependent mechanisms regulate synaptic growth and function. Nature 2001;412:449â452. [PubMed: 11473321]

DiAntonio A, Hicke L. Ubiquitin-dependent regulation of the synapse. Annu Rev Neurosci 2004;27:223â246. [PubMed: 15217332]

Egger MD, Nowakowski RS, Peng B, Wyman RJ. Patterns of connectivity in a Drosophila nerve. J Comp Neurol 1997;387:63â72. [PubMed: 9331172]

Gao FB, Kohwi M, Brenman JE, Jan LY, Jan YN. Control of dendritic field formation in Drosophila: the roles of flamingo and competition between homologous neurons. Neuron 2000;28:91â101. [PubMed: 11086986]

Goda Y, Davis GW. Mechanisms of synapse assembly and disassembly. Neuron 2003;40:243â264. [PubMed: 14556707]

Harmar AJ. Family-B G-protein-coupled receptors. Genome Biol 2001;2:3013.1â3013.10.

Hatada Y, Wu F, Silverman R, Schacher S, Goldberg DJ. En passant synaptic varicosities form directly from growth cones by transient cessation of growth cone advance but not of actin-based motility. J Neurobiol 1999;41:242â251. [PubMed: 10512981]

Hill E, Broadbent ID, Chothia C, Pettitt J. Cadherin superfamily proteins in Caenorhabditis elegans and Drosophila melanogaster. J Mol Biol 2001;305:1011â1024. [PubMed: 11162110]

Hoang B, Chiba A. Single-cell analysis of Drosophila larval neuromuscular synapses. Dev Biol 2001;229:55â70. [PubMed: 11133154]

Hummel T, Krukkert K, Roos J, Davis G, Klambt C. Drosophila Futsch/22C10 is a MAP1B-like protein required for dendritic and axonal development. Neuron 2000;26:357â370. [PubMed: 10839355]

Hurd DD, Saxton WM. Kinesin mutations cause motor neuron disease phenotypes by disrupting fast axonal transport in Drosophila. Genetics 1996;144:1075â1085. [PubMed: 8913751]

Jan LY, Jan YN. Properties of the larval neuromuscular junction in Drosophila melanogaster. J Physiol 1976;262:189â214. [PubMed: 11339]

Jan LY, Jan YN. Antibodies to horseradish peroxidase as specific neuronal markers in Drosophila and in grasshopper embryos. Proc Natl Acad Sci U S A 1982;79:2700â2704. [PubMed: 6806816]

Jefferis GS, Marin EC, Stocker RF, Luo L. Target neuron prespecification in the olfactory map of Drosophila. Nature 2001;414:204â208. [PubMed: 11719930]

Jia XX, Gorczyca M, Budnik V. Ultrastructure of neuromuscular junctions in Drosophila: comparison of wild type and mutants with increased excitability. J Neurobiol 1993;24:1025â1044. [PubMed: 8409967]

Keshishian H, Broadie K, Chiba A, Bate M. The drosophila neuromuscular junction: a model system for studying synaptic development and function. Annu Rev Neurosci 1996;19:545â575. [PubMed: 8833454]

Keshishian H, Kim YS. Orchestrating development and function: retrograde BMP signaling in the Drosophila nervous system. Trends Neurosci 2004;27:143â147. [PubMed: 15036879]

Kopczynski CC, Davis GW, Goodman CS. A neural tetraspanin, encoded by late bloomer, that facilitates synapse formation. Science 1996;271:1867â1870. [PubMed: 8596956]

Lee RC, Clandinin TR, Lee CH, Chen PL, Meinertzhagen IA, Zipursky SL. The protocadherin Flamingo is required for axon target selection in the Drosophila visual system. Nat Neurosci 2003;6:557â563. [PubMed: 12754514]

Lu B, Usui T, Uemura T, Jan L, Jan YN. Flamingo controls the planar polarity of sensory bristles and asymmetric division of sensory organ precursors in Drosophila. Curr Biol 1999;9:1247â1250. [PubMed: 10556092]

Luo L, O'leary DD. Axon retraction and degeneration in development and disease. Annu Rev Neurosci 2005;28:127â156. [PubMed: 16022592]

Mackler JM, Drummond JA, Loewen CA, Robinson IM, Reist NE. The C(2)B Ca(2+)-binding motif of synaptotagmin is required for synaptic transmission in vivo. Nature 2002;418:340â344. [PubMed: 12110842]

Marques G, Bao H, Haerry TE, Shimell MJ, Duchek P, Zhang B, O'Connor MB. The Drosophila BMP type II receptor Wishful Thinking regulates neuromuscular synapse morphology and function. Neuron 2002;33:529â543. [PubMed: 11856528]

Marrus SB, Portman SL, Allen MJ, Moffat KG, DiAntonio A. Differential localization of glutamate receptor subunits at the Drosophila neuromuscular junction. J Neurosci 2004;24:1406â1415. [PubMed: 14960613]

Martin M, Iyadurai SJ, Gassman A, Gindhart JG Jr, Hays TS, Saxton WM. Cytoplasmic dynein, the dynactin complex, and kinesin are interdependent and essential for fast axonal transport. Mol Biol Cell 1999;10:3717â3728. [PubMed: 10564267]

McCabe BD, Marques G, Haghighi AP, Fetter RD, Crotty ML, Haerry TE, Goodman CS, O'Connor MB. The BMP homolog Gbb provides a retrograde signal that regulates synaptic growth at the Drosophila neuromuscular junction. Neuron 2003;39:241â254. [PubMed: 12873382]

Monastirioti M, Gorczyca M, Rapus J, Eckert M, White K, Budnik V. Octopamine immunoreactivity in the fruit fly Drosophila melanogaster. J Comp Neurol 1995;356:275â287. [PubMed: 7629319]

Murphey RK, Godenschwege TA. New roles for ubiquitin in the assembly and function of neuronal circuits. Neuron 2002;36:5â8. [PubMed: 12367500]

Nishikawa K, Kidokoro Y. Octopamine inhibits synaptic transmission at the larval neuromuscular junction in Drosophila melanogaster. Brain Res 1999;837:67â74. [PubMed: 10433989]

Oh CE, McMahon R, Benzer S, Tanouye MA. bendless, a Drosophila gene affecting neuronal connectivity, encodes a ubiquitin-conjugating enzyme homolog. J Neurosci 1994;14:3166â3179. [PubMed: 8182464]

Packard M, Mathew D, Budnik V. Wnts and TGF beta in synaptogenesis: old friends signalling at new places. Nat Rev Neurosci 2003;4:113â120. [PubMed: 12563282]

Raff MC, Whitmore AV, Finn JT. Axonal self-destruction and neurodegeneration. Science 2002;296:868â871. [PubMed: 11988563]

Rawson JM, Lee M, Kennedy EL, Selleck SB. Drosophila neuromuscular synapse assembly and function require the TGF-beta type I receptor saxophone and the transcription factor Mad. J Neurobiol 2003;55:134â150. [PubMed: 12672013]

Reuter JE, Nardine TM, Penton A, Billuart P, Scott EK, Usui T, Uemura T, Luo L. A mosaic genetic screen for genes necessary for Drosophila mushroom body neuronal morphogenesis. Development 2003;130:1203â1213. [PubMed: 12571111]

Roos J, Hummel T, Ng N, Klambt C, Davis GW. Drosophila Futsch regulates synaptic microtubule organization and is necessary for synaptic growth. Neuron 2000;26:371â382. [PubMed: 10839356]

Roos J, Kelly RB. The endocytic machinery in nerve terminals surrounds sites of exocytosis. Curr Biol 1999;9:1411â1414. [PubMed: 10607569]

Ruthazer ES, Cline HT. Insights into activity-dependent map formation from the retinotectal system: a middle-of-the-brain perspective. J Neurobiol 2004;59:134â146. [PubMed: 15007832]

Senti KA, Usui T, Boucke K, Greber U, Uemura T, Dickson BJ. Flamingo regulates R8 axon-axon and axon-target interactions in the Drosophila visual system. Curr Biol 2003;13:828â832. [PubMed: 12747830]

Shapira M, Zhai RG, Dresbach T, Bresler T, Torres VI, Gundelfinger ED, Ziv NE, Garner CC. Unitary assembly of presynaptic active zones from Piccolo-Bassoon transport vesicles. Neuron 2003;38:237â252. [PubMed: 12718858]

Shima Y, Kengaku M, Hirano T, Takeichi M, Uemura T. Regulation of dendritic maintenance and growth by a mammalian 7-pass transmembrane cadherin. Dev Cell 2004;7:205â216. [PubMed: 15296717]

Stewart BA, Atwood HL, Renger JJ, Wang J, Wu CF. Improved stability of Drosophila larval neuromuscular preparations in haemolymph-like physiological solutions. J Comp Physiol [A] 1994;175:179â191.

Stowers RS, Schwarz TL. A genetic method for generating Drosophila eyes composed exclusively of mitotic clones of a single genotype. Genetics 1999;152:1631â1639. [PubMed: 10430588]

Sweeney NT, Li W, Gao FB. Genetic manipulation of single neurons in vivo reveals specific roles of flamingo in neuronal morphogenesis. Dev Biol 2002;247:76â88. [PubMed: 12074553]

Tai MH, Zipser B. Sequential steps in synaptic targeting of sensory afferents are mediated by constitutive and developmentally regulated glycosylations of CAMs. Dev Biol 1999;214:258â276. [PubMed: 10525333]

Tepass U, Truong K, Godt D, Ikura M, Peifer M. Cadherins in embryonic and neural morphogenesis. Nat Rev Mol Cell Biol 2000;1:91â100. [PubMed: 11253370]

Tessier-Lavigne M, Goodman CS. The molecular biology of axon guidance. Science 1996;274:1123â1133. [PubMed: 8895455]

Tissir F, Bar I, Jossin Y, Goffinet AM. Protocadherin Celsr3 is crucial in axonal tract development. Nat Neurosci 2005;8:451â457. [PubMed: 15778712]

Usui T, Shima Y, Shimada Y, Hirano S, Burgess RW, Schwarz TL, Takeichi M, Uemura T. Flamingo, a seven-pass transmembrane cadherin, regulates planar cell polarity under the control of Frizzled. Cell 1999;98:585â595. [PubMed: 10490098]

Wagh DA, Rasse TM, Asan E, Hofbauer A, Schwenkert I, Durrbeck H, Buchner S, Dabauvalle MC, Schmidt M, Qin G, Wichmann C, Kittel R, Sigrist SJ, Buchner E. Bruchpilot, a protein with homology to ELKS/CAST, is required for structural integrity and function of synaptic active zones in Drosophila. Neuron 2005;49:833â844. [PubMed: 16543132]

Wan HI, DiAntonio A, Fetter RD, Bergstrom K, Strauss R, Goodman CS. Highwire regulates synaptic growth in Drosophila. Neuron 2000;26:313â329. [PubMed: 10839352]

Wang X, Weiner JA, Levi S, Craig AM, Bradley A, Sanes JR. Gamma protocadherins are required for survival of spinal interneurons. Neuron 2002;36:843â854. [PubMed: 12467588]

Washbourne P, Dityatev A, Scheiffele P, Biederer T, Weiner JA, Christopherson KS, El-Husseini A. Cell adhesion molecules in synapse formation. J Neurosci 2004;24:9244â9249. [PubMed: 15496659]

Weiner JA, Wang X, Tapia JC, Sanes JR. Gamma protocadherins are required for synaptic development in the spinal cord. Proc Natl Acad Sci U S A 2005;102:8â14. [PubMed: 15574493]

Wu MN, Fergestad T, Lloyd TE, He Y, Broadie K, Bellen HJ. Syntaxin 1A interacts with multiple exocytic proteins to regulate neurotransmitter release in vivo. Neuron 1999;23:593â605. [PubMed: 10433270]Erratum in: Neuron 2000 25:735

Zhang B, Koh YH, Beckstead RB, Budnik V, Ganetzky B, Bellen HJ. Synaptic vesicle size and number are regulated by a clathrin adaptor protein required for endocytosis. Neuron 1998;21:1465â1475. [PubMed: 9883738]

Zinsmaier KE, Eberle KK, Buchner E, Walter N, Benzer S. Paralysis and early death in cysteine string protein mutants of Drosophila. Science 1994;263:977â980. [PubMed: 8310297]

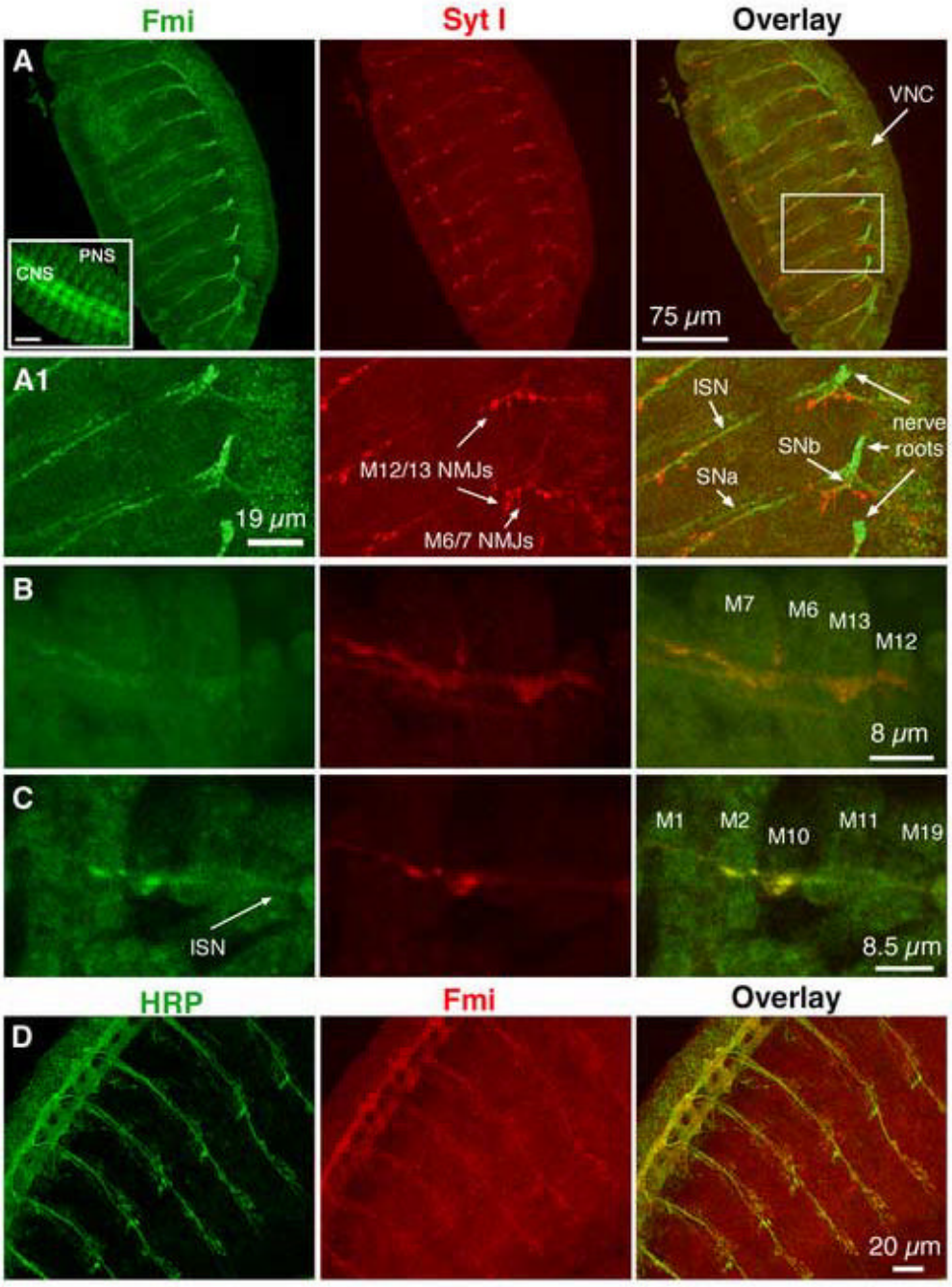

Figure 1.

Flamingo is expressed in motor axons and presynaptic terminals

(A & A1). A confocal image of segmental nerve projection and presynaptic terminals on the bodywall muscle in a wild type embryo. The boxed area in panel A is enlarged below (A1). The nerve roots exiting the ventral nerve cord (VNC) of the central nervous system (CNS) are clearly immunoreactive to a Flamingo mAB (Fmi, green). The intersegmental nerve (ISN), segmental nerves SNa and SNb (indicated by arrows) are also stained for Flamingo. At this view level, presynaptic terminals at the NMJ are marked by a polyclonal Ab to the synaptic vesicle synaptotagmin I (Syt I, red). At NMJs, synaptotagmin I is enriched at the tip of axons. Further, synaptotagmin I immunoreactivity partially overlaps with Flamingo staining. The

inset in panel A (left corner) shows Flamingo expression in both CNS and sensory cells in the peripheral nervous system (PNS). All embryos used in this and the following panels were approximately 18 hrs old.

(B & C). In dissected embryonic bodywall muscles, Flamingo is detected weakly in muscles but at slightly higher levels in axons and presynaptic terminals.

(D). The immunoreactivity for HRP (green, a neuronal membrane marker) and Flamingo (red) is found on the same CNS and axonal projections

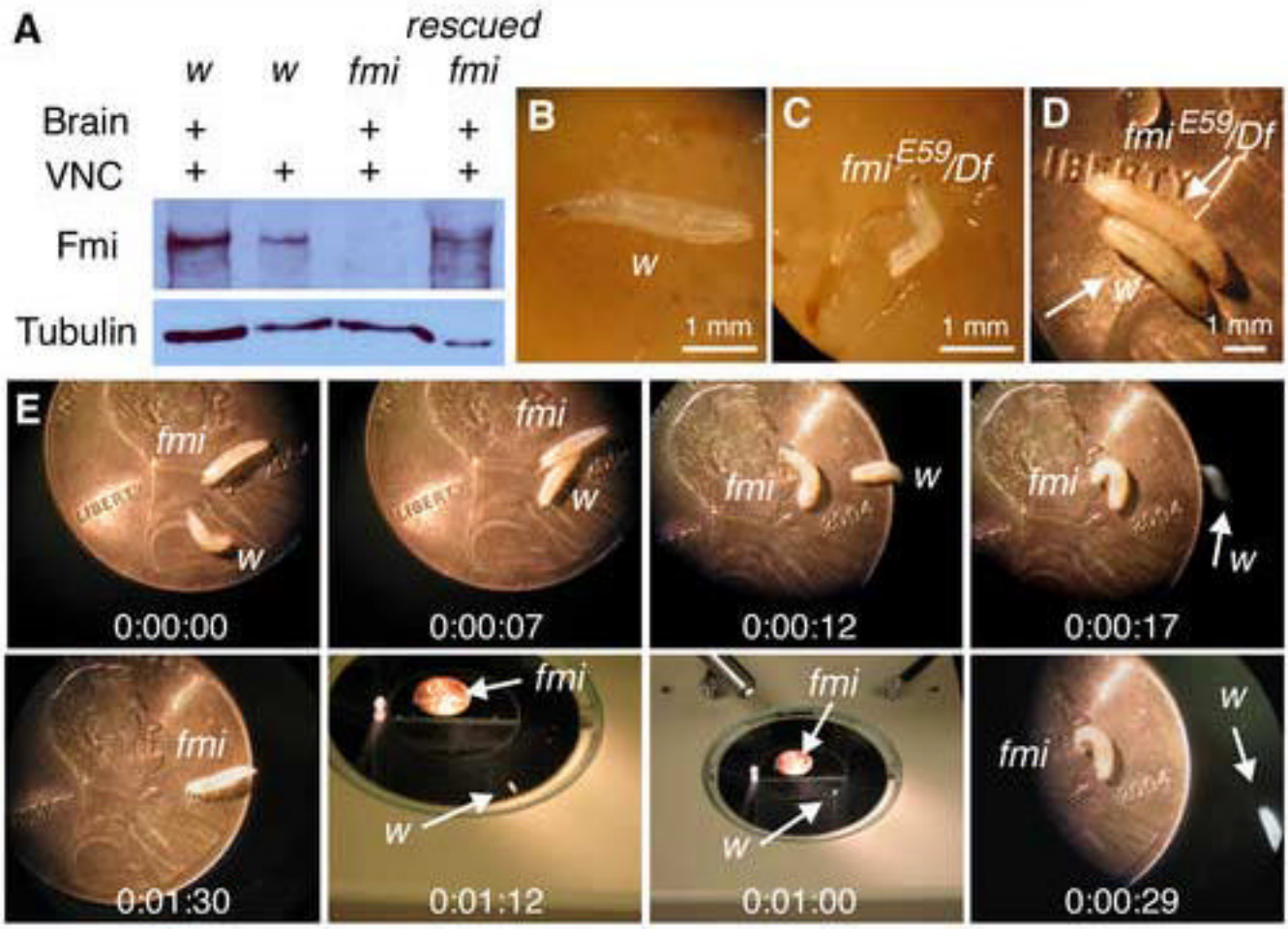

Figure 2.

Western blot of Flamingo in the larval CNS and the growth and locomotion of *fmi* mutant larvae

(A). A Western blot of 3rd instar larval CNS (brain + VNC) or VNC in wild type (*w*), *fmi* mutant (*fmi*^{E59}/*Df*), and rescued *fmi* mutant (*fmi*^{E59}, Elav Gal4/*fmi*^{72}, UAS-Fmi) is probed with a Flamingo antibody (upper panel). In a duplicated gel, an antibody to tubulin is used to examine the protein loading level. Note the presence of Flamingo in both CNS and VNC in the wild type and the rescued mutant and its absence in the *fmi* mutant.

(B & C). Photographs of 3rd instar larvae in the wild type and the *fmi* mutant 7 days after hatching from the egg case. Note that the mutant larva is smaller in body size compared to the wild type.

(D). Within additional 4-7 days, the mutant larva continues to forage in the food and grows to mature wandering 3rd instar larva, whose body size is larger than that of its wild type counterpart.

(E). Still photographs illustrate the locomotion of the wild type larva and the mutant larva from panel D. The wild type larva quickly wanders off the penny, whereas the mutant larva crawls slowly.

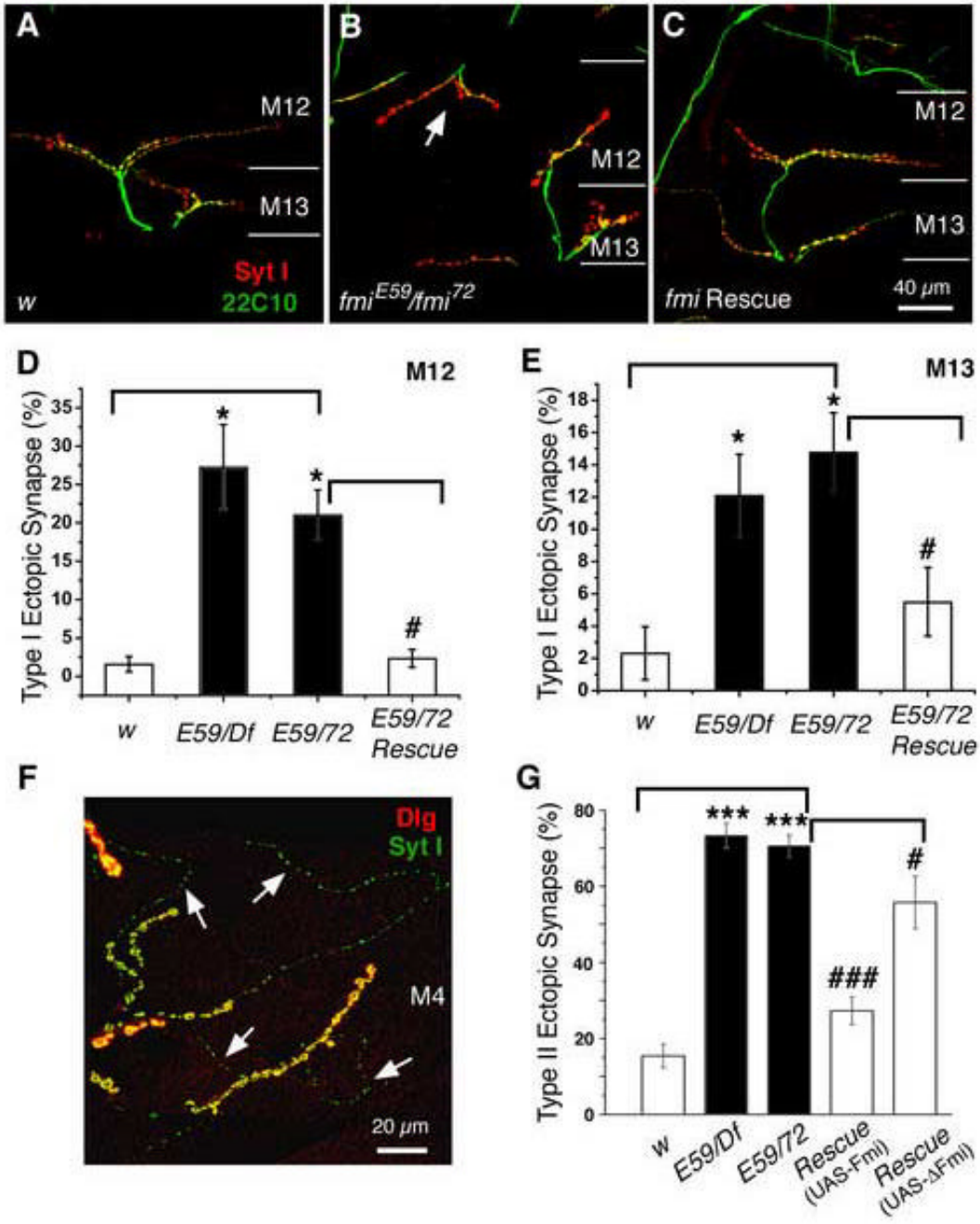

Figure 3.

Mutations in *fmi* cause a significant increase in the number of ectopic type I boutons **(A-C).** Representative immunocytochemical staining of the NMJs on muscles 12 and 13 with antibodies to the synaptic vesicle protein synaptotagmin I (Syt I, red) and the microtubule-associated protein Futsch (22C10, green) in the control (*w*, **A**), the fmi^{E59}/fmi^{72} (**B**), and rescued fmi^{E59}/fmi^{72} (**C**) larvae. Ectopic type I synapses on muscle 12 are indicated by the arrows in panel (**B**). The while lines mark the boundary between muscles 12 and 13.
(D & E). Histograms show that *fmi* mutations significantly increase the fraction of muscles (muscle 12, **D** and muscle 13, **E**) receiving ectopic type I synapses compared to that in the *w*

control larvae (* $p<0.05$). This defect is effectively rescued by neuronal expression of the wild type Flamingo in the fmi^{E59}/fmi^{72} mutant background (# $p<0.05$).

(F). A representative image showing ectopic type II innervations on muscle 4 in *fmi* mutants labeled with the postsynaptic marker Dlg (red) and presynaptic marker Syt I (green). Type II synaptic boutons are marked by arrows.

(G). Histogram plots show that the percentage of muscle 4 receiving ectopic type II synaptic input is significantly increased in fmi^{E59}/Df and fmi^{E59}/fmi^{72} mutant larvae (***$P<0.001$). This defect can be effectively rescued to near wild type levels by neuronal expression of the wild type Flamingo in the fmi^{E59}/fmi^{72} mutant background, but only partially rescued by expression of the truncated Flamingo (### $p<0.001$; # $P<0.05$).

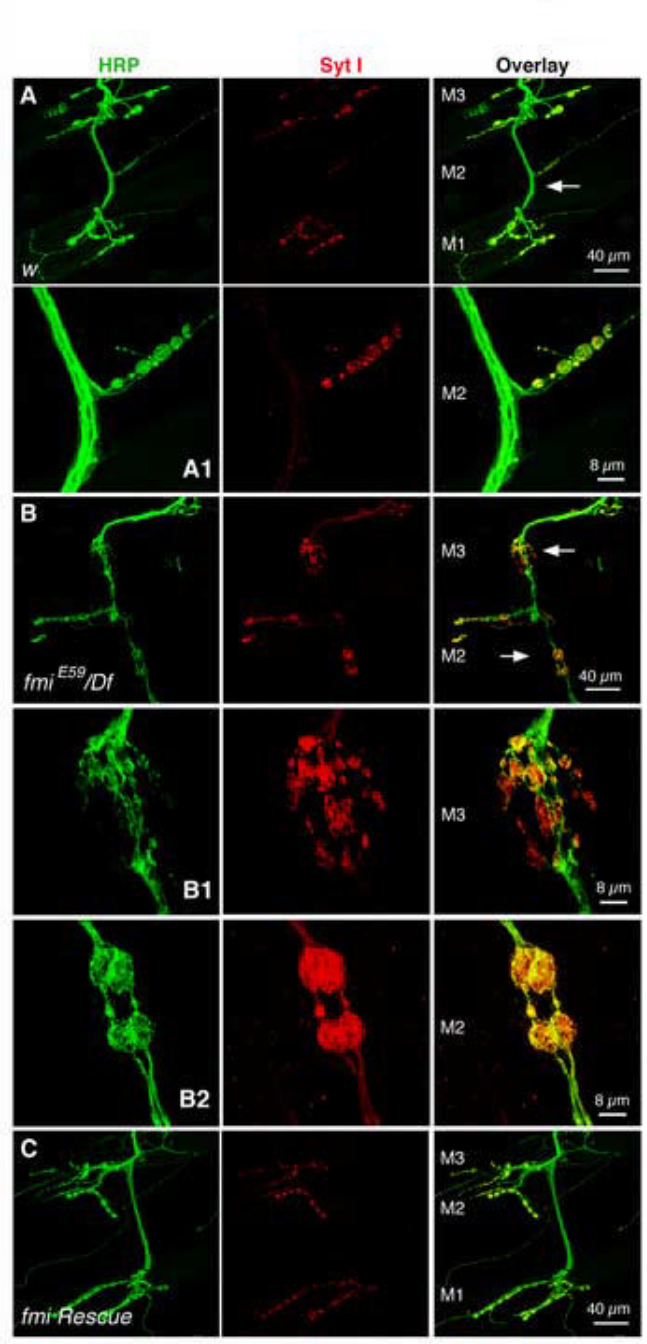

Figure 4.

En passant synapses are found on muscles 2 and 3 in the *fmi* mutant

(A & A1). Representative images of axons (HRP, green) and synapses (Syt I, red) on muscles 1, 2 and 3 in the control larvae (**A**). The NMJ indicated by the arrow is shown at higher magnification in panel (**A1**). Note the usual âbeads-on-a-stringâ pattern of synaptic boutons extended on the muscle surface.

(B-B2). Representative images of axons (HRP, green) and synapses (Syt I, red) on muscles 2 and 3 in the fmi^{E59}/Df larvae (**B**). The NMJs indicated by the arrows are shown at higher magnification below in panels (**B1**) and (**B2**). Compared to the NMJ in the control larva, these axons arrive on muscles 2 and 3 as one bundle, then defasciculate into individual axons and

form boutons along the axon on muscles 2 and 3, and finally converge back to one nerve bundle and proceed to the next muscle. Synaptic vesicle proteins represented by Syt I are well retained within each *en passant* synapse. Note the irregular sized, often enlarged, synaptic boutons. **(C).** The formation of these *en passant* synapses can be partially suppressed by neuronal expression of the wild type Flamingo in the mutant background.

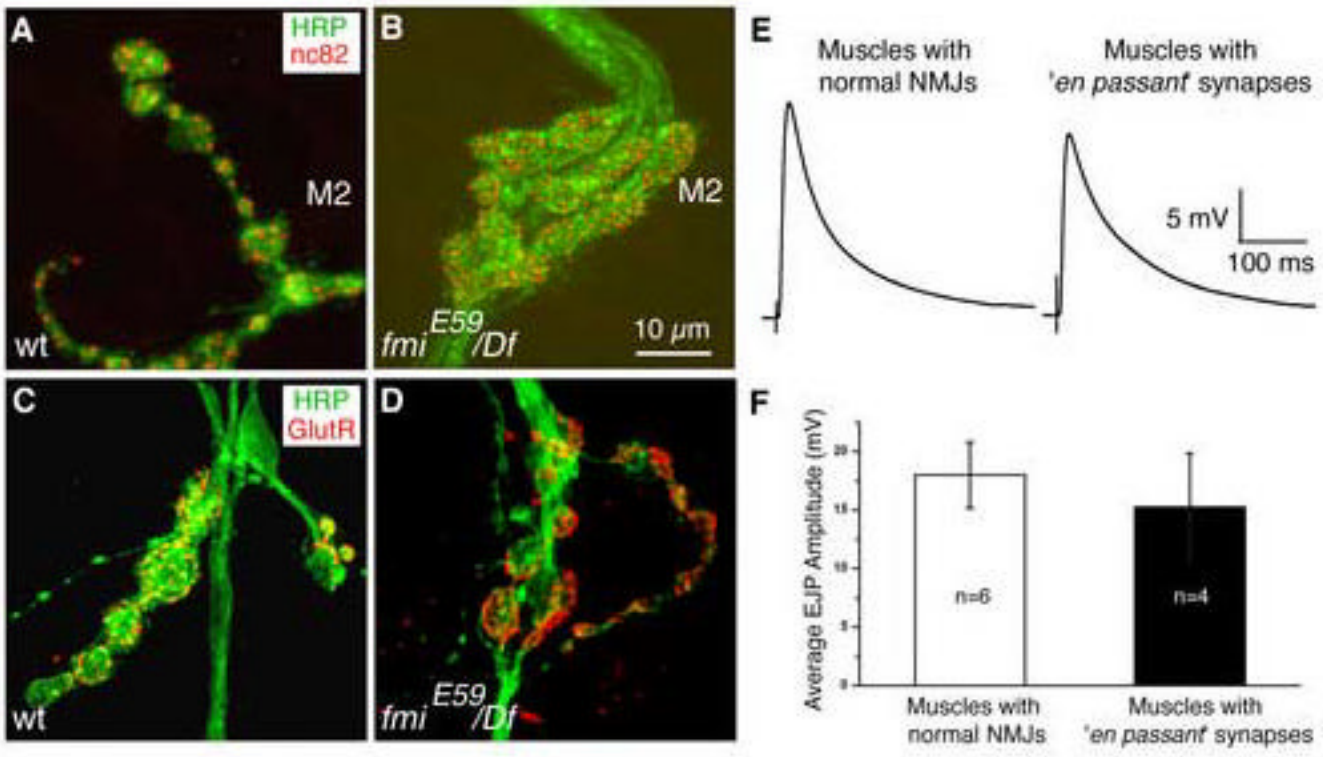

Figure 5.

The *en passant* synapse contains presynaptic active zones and postsynaptic glutamate receptors and functions normally

(A, B). Representative images of NMJs on muscle 2 stained for neuronal membranes (HRP, green) and active zones (nc82, red) in the wildtype larvae (panel A) and fmi^{E59}/Df mutant larvae (panel B).

(C, D). Representative images of NMJs on muscle 2 stained for neuronal membranes (HRP, green) and glutamate receptor III (red) in the wildtype larva (panel C) and fmi^{E59}/Df mutant larva (panel D).

(E, F). Representative EJPs from muscles with normal NMJs (panel E, left) and from muscles with â*en passant*â synapses (panel E, right) in fmi^{E59}/Df mutant larvae. The average amplitude of EJPs is slightly reduced in muscles with the â*en passant*â synapse (panel F); however, this reduction is not statistically significant.

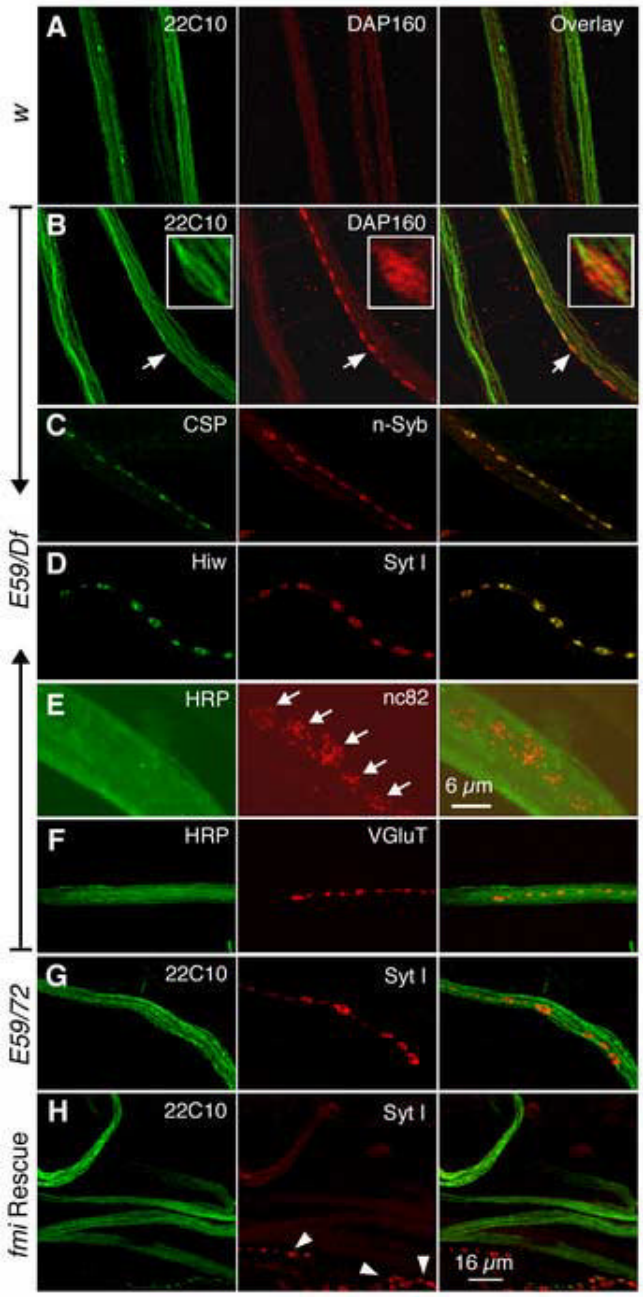

Figure 6.

Axonal varicosities are found within the segmental nerve of the *fmi* mutant

(A, B). Representative images of colocalization of the microtubule-associated protein Futsch (22C10, green) and the endocytotic protein DAP160 (red) on segmental nerves of control larvae (**A**) and fmi^{E59}/Df mutant larvae (**B**), respectively. Note that DAP160 is present at low levels uniformly along the control segmental nerve. In contrast, some segmental nerves similar to the one shown in panels (**B**) have a string of bouton-like varicosities clustered on axons. Insets show one of the axonal varicosities at higher magnification.

(C-F). Representative images showing colocalization of various synaptic (Hiw, nc82) and synaptic vesicle proteins (CSP, n-Syb, Syt I, VGluT) along segmental nerves of the *fmi* mutant

larvae. Panels (**C**) show that the synaptic vesicle protein cysteine-string protein (CSP, green) colocalizes with the synaptic vesicle protein neuronal synaptobrevin (n-Syb, red) within the string of bouton-like varicosities along the segmental nerve. Panels (**D**) show that the peri-active zone protein Highwire (Hiw, green) colocalizes with the synaptic vesicle protein synaptotagmin I (Syt I, red) within the bouton-like varicosities. Panels (**E**) show that the active zone marker nc82 is clustered in bouton-like shapes along the segmental nerve (marked by HRP). Panels (**F**) show the localization of the Drosophila vesicular glutamate transporter (VGluT) along the segmental nerve (marked by HRP).

(G & H). The axonal varicosities found in the fmi^{E9}/fmi^{72} mutant (**G**) can be rescued by neuronal expression of the wild type Flamingo in the mutant background (**F**). Note the absence of Syt I-positive varicosities along the segmental nerve in the rescued *fmi* mutant. Arrowheads point to synaptic boutons normally found on bodywall muscles. However, this rescue is statistically significant but not a full rescue (see Fig. S3E).

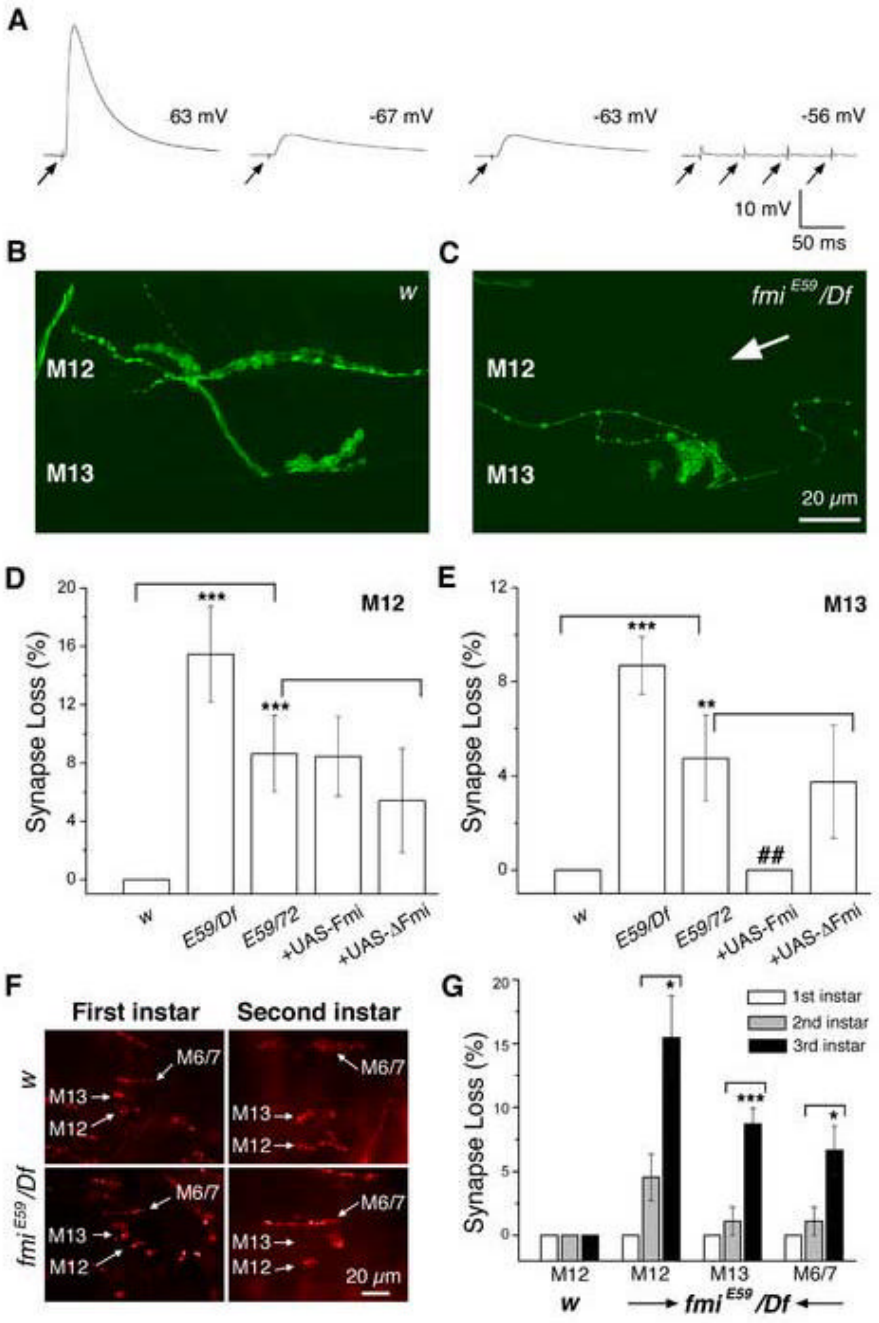

Figure 7.

The *fmi* mutant loses synaptic potentials and displays an age-dependent loss of NMJs

(A). Examples of muscles in 3rd instar *fmi* mutant larvae that display normal (the first example of EJP), dramatically reduced (the 2nd and 3rd examples of EJPs) or no synaptic potentials (the last example, with four arrows) evoked by stimulating the segmental nerve. The resting potential of each muscle is shown. These recordings were conducted under identical experimental conditions and in HL-3 saline containing 1 mM Ca^{2+}. Arrows indicate the onset of nerve stimulation. Note that multiple stimuli failed to evoke any synaptic response in the last muscle.

(B, C). Representative images of NMJs on muscles 12 and 13 (stained for HRP, green) in the control (**B**) and *fmi*^{E59}/*Df* larvae (**C**) at the 3rd instar stage. An example of muscle 12 that has lost its normal NMJ is shown here (see arrow in panel **C**).

(D, E). Histograms of the percentage of muscles 12 (**D**) and 13 (**E**) that are denervated in 3rd instar larvae. While the control larvae have normal NMJs in all cases tested, *fmi* mutants have a significant number of muscles that lack synaptic inputs. These defects can be effectively rescued by expressing the wild type Flamingo in the *fmi*^{E59}/ *fmi*^{72} mutant background in muscle 13, but not fully in muscle 12 ($p>0.05$). Expression of the truncated Flamingo lacking most of the extracellular domain does not rescue these defects. *fmi* mutants (*fmi*^{E59}/*Df*, and *fmi*^{E59}/ *fmi*^{72}) have significantly more muscles that lost NMJs compared to that in *w* control larvae (*** $p<0.001$; ** $p<0.01$; panel **D**). The rescued mutants (*fmi*^{E59}/ *fmi*^{72} + wild type Flamingo) have significantly fewer muscles that lost NMJs compared to that in *fmi*^{E59}/ *fmi*^{72} mutants (## $p<0.01$; panel **E**).

(F). Representative images of NMJs on ventral muscles (muscles 6, 7, 12 and 13) in 1st and 2nd instar larvae of the control fly (*w*, **top panels**) and the *fmi* mutant (**bottom panels**).

(G). Histograms comparing the percentage of muscles that do not have NMJs in 1st, 2nd and 3rd instar larvae. Note the absence of synapse loss in 1st instar mutant larva and the increase in synapse loss from 2nd instar larvae to 3rd instar larvae. * $p<0.05$; *** $p<0.001$;

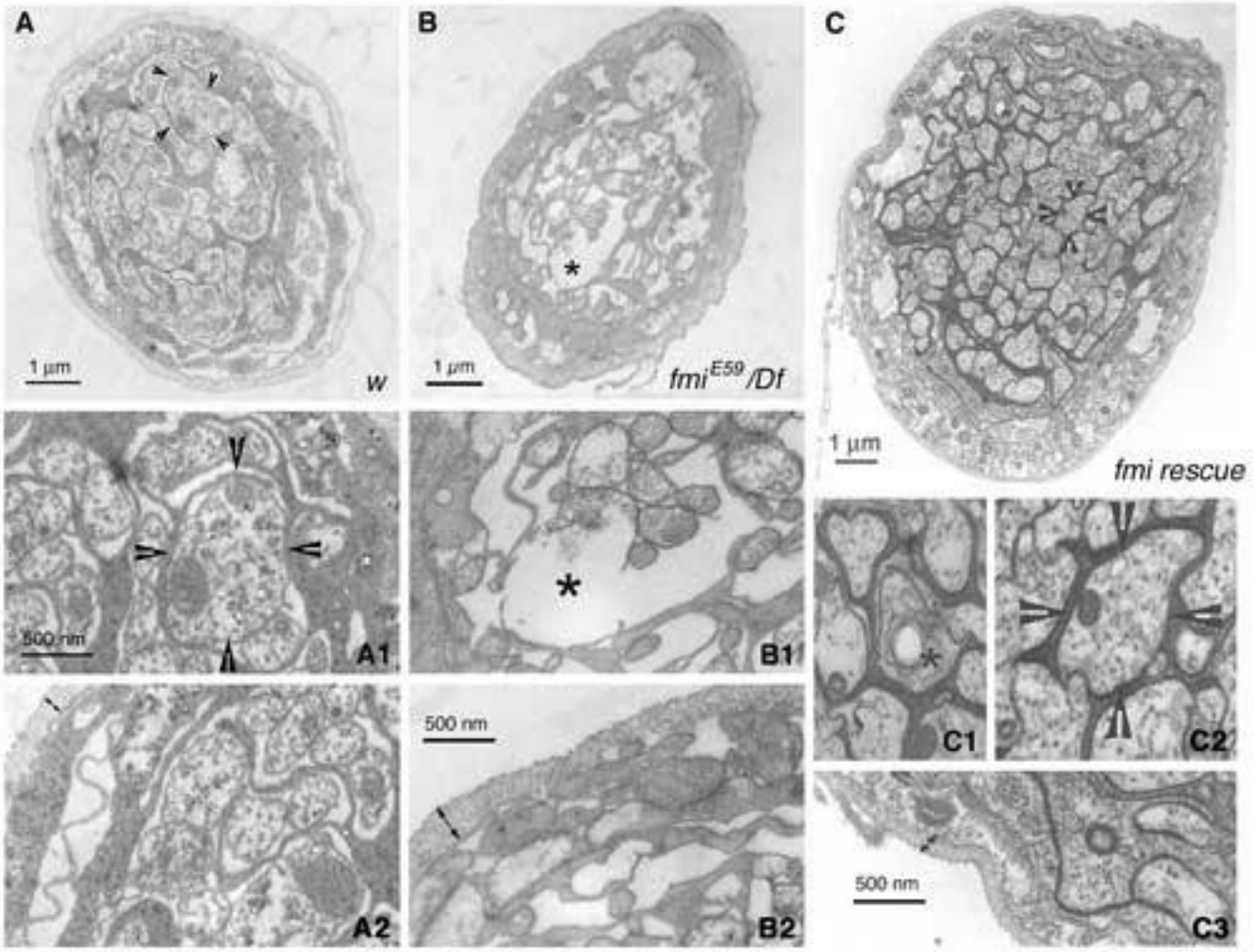

Figure 8.

Axonal degeneration of segmental nerves in the *fmi* mutant larvae and its rescue by neuronal expression of Flamingo

(A-A2). Panel (**A)** shows a representative cross-section of the segmental nerve from a control (*w*) larva. The arrowheads point to one axon that is further magnified in panel (**A1**). Axons are packed with mitochondria and microtubules. The edge of the segmental nerve is magnified in panel (**A2**) to illustrate the thickness of the neuronal sheath (double headed arrows).

(B-B2). Panel (**B**) shows a representative cross-section of the segmental nerve for an fmi^{E59}/*Df* mutant larva. In contrast to panel (**A**), the mutant nerve has more empty âholesâ and is relatively less packed with axons and glial processes. The asterisk marks the gap in the nerve that is magnified in panel (**B1**). These axons are less packed with mitochondria and microtubules. Double-headed arrows in panel (**B2**) delimit the sheath surrounding the segmental nerves of the mutant. Note the thickening of the nerve sheath.

(C-C3). Panel (**C**) shows a representative cross-section of the segmental nerve for an fmi^{E59}/*Df* mutant larva rescued by expressing a wild type Flamingo in postmitotic neurons. In contrast to panel (**B**), the rescued nerve is larger in diameter and well packed with axons and glial processes. The asterisk marks one axon undergoing degeneration that is magnified in panel (**C1**). The arrowheads point to one axon that is further magnified in panel (**C2**). Similar to axons in the wild type, the rescued axons are packed with mitochondria and microtubules.

Double-headed arrows in panel (**C3**) delimit the sheath surrounding the segmental nerves of the rescued larva. Note that the nerve sheath is restored to the thickness found in the wild type.

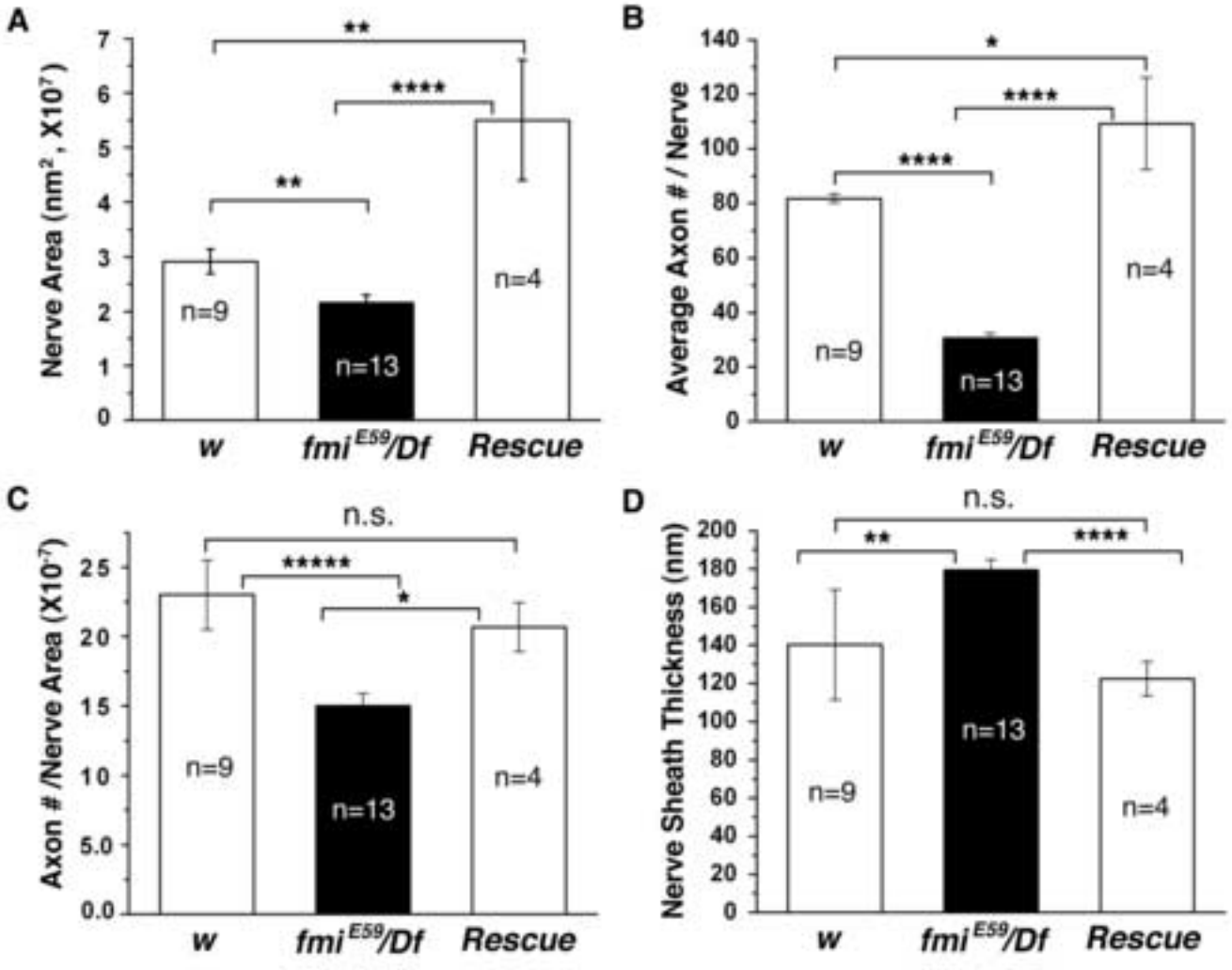

Figure 9.

Summary of morphological properties of segmental nerves in the wild type, *fmi* mutant, and rescued mutant larvae

(A). The average area of the segmental nerve is significantly reduced in the fmi^{E59}/Df mutant. In rescued mutant larvae, the segmental nerve is significantly enlarged. *p<0.05; **p<0.01; ****p<<0.001 (the same below).

(B). The average number of axons per segmental nerve is significantly reduced in the fmi^{E59}/Df mutant. In rescued larvae, each segmental nerve has slightly more numbers of axons.

(C). The average number of axons per area of the segmental nerve is significantly reduced in the fmi^{E59}/Df mutant. This is completely rescued to wild type levels in rescued larvae. n.s. = not significantly different.

(D). The average thickness of the nerve sheath surrounding the segmental nerve is significantly increased in the fmi^{E59}/Df mutant. This defect is fully corrected in rescued larvae. n.s. = not significantly different. Data are expressed as Mean values Â S.E.M.